

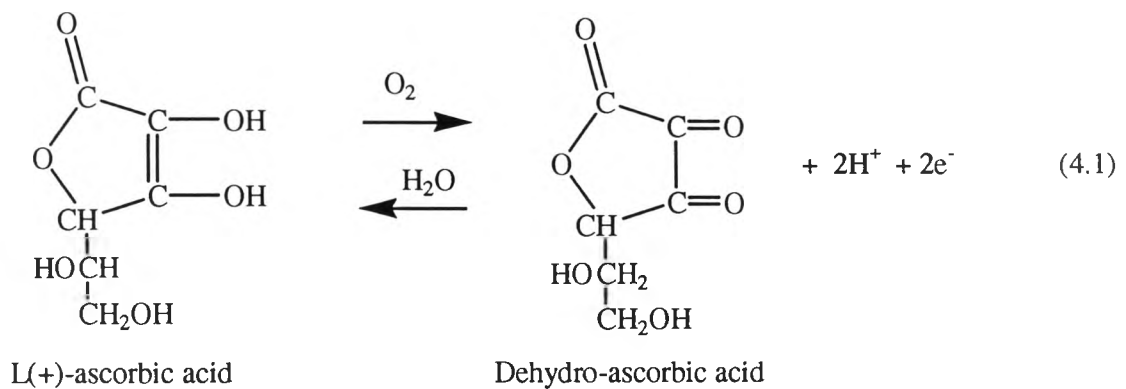
CHAPTER IV

RESULTS AND DISCUSSION

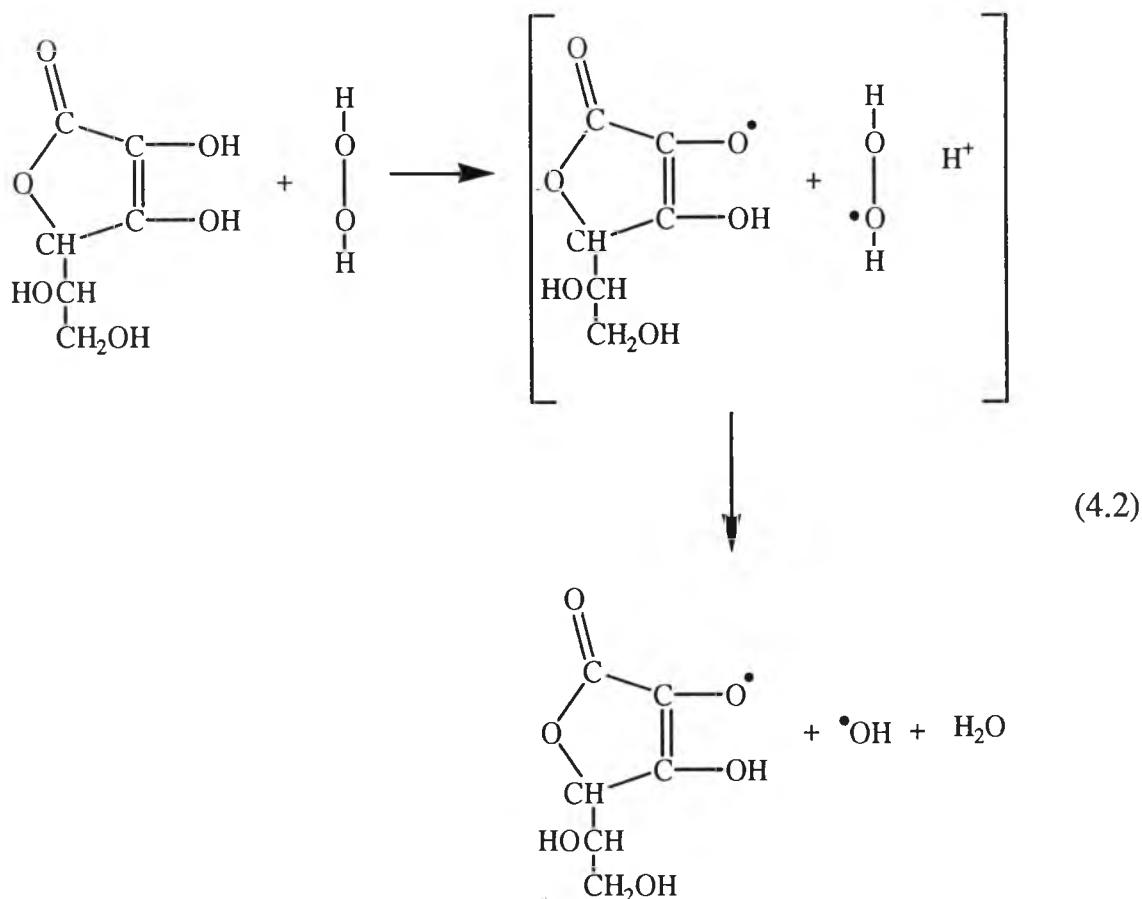
Based on the previous work of Arayamaythalert [2, 44], native cassava starch was chemically modified into starch graft poly(acrylic acid) under a grafting copolymerization of acrylic onto the polysaccharide backbone via a hydrogen peroxide-ascorbic acid initiation method. This mechanism is shown below:

1) Redox System

This method used a reducing agent of L(+)-ascorbic acid as an accelerator for hydrogen peroxide. In aqueous system, ascorbic acid is reversibly oxidized to dehydro-ascorbic as shown in Equation 4.1



Apparently this redox reaction proceeds by two successive one-electron transfer reaction, which suggests that its chemical property is responsible for its accelerative action with hydrogen peroxide. The free radicals (R[•]) are created by this method. A possible proton-assisted one electron transfer mechanism for an oxidation reaction is shown in Equation 4.2.



Increasing the reaction temperature is to cause a faster rate of hydrogen peroxide decomposition to water and oxygen gas. The oxygen molecules can then oxidize L(+)-ascorbic acid to dehydroascorbic acid, a non reactive species for the graft polymerization as shown in Equation 4.1.

The number of free radicals is responsible for the relative amounts of homopolymer and copolymer. The homopolymerization and graft polymerization take place simultaneously and competitively.

2) Homopolymerization [2]

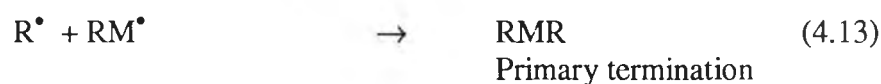




3) Graft polymerization



4) Radical termination



In this thesis, the starch-g-poly(acrylic acid) was synthesized in order to search the appropriate thickener for water-based screen inks printed on plastic film. Water absorption capacity and rheological properties of the modified starch were carried out using different crosslinking concentrations.

4.1 The Effect of Crosslinking Concentration on Water Absorption Capacity of Starch-g-Poly(acrylic acid)

The effect of the crosslinking agent (*N,N'*-MBA) concentration (% weight based on the total of acrylic acid) on water absorption capacity of saponified starch-g-poly(acrylic acid) copolymer is presented in Table 4.1 and Figure 4.1, respectively.

Table 4.1 Effect of the Crosslinking Agent Concentration on Water Absorption Capacity of Saponified Starch-g-Poly(acrylic acid) Copolymer

<i>N,N'</i> -MBA (wt%)	Water Absorption in Distilled Water (g g^{-1})
0.5	34 ± 2
1.0	73 ± 5
1.5	74 ± 2
2.0	86 ± 6
2.5	90 ± 2

Data were obtained under the following condition: starch = 60 g, $[\text{H}_2\text{O}_2] = 4 \text{ cm}^3$, ascorbic acid = 0.4 g, acrylic acid = 80 cm^3 , reaction temperature = 35°C, reaction time = 2 hours.

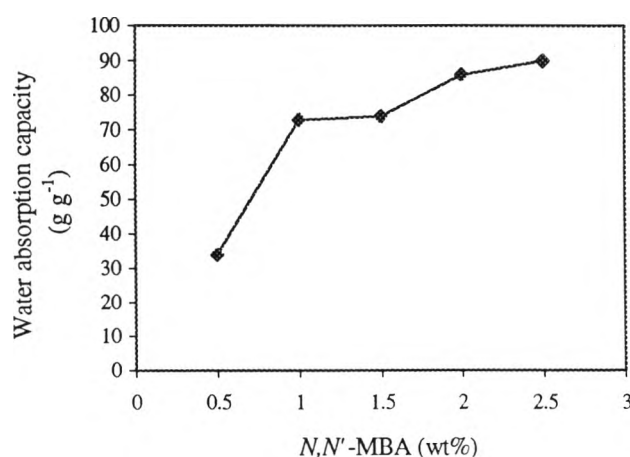


Figure 4.1 Effect of *N,N'*-MBA concentration on water absorption capacity of saponified starch-g-poly(acrylic acid) copolymer

From Table 4.1, the experiment data show that the water absorption capacity increases with increasing the amount of crosslinker. For that reason, the homopolymer is soluble in the aqueous medium while the crosslinker reduces the water solubility of polymer by the crosslinking reaction. This means that increase the crosslinking agent concentration leads to increase the crosslinked points [45], which decrease the opportunity of homopolymerization reaction according to Equations 4.3-4.6.

From Figure 4.1, the graft copolymer which gave the minimum water absorption capacity was synthesized with 0.5 wt% of *N,N'*-MBA. The water absorption of graft copolymer rises significantly with increases of the crosslinking agent concentration from 0.5 to 1.0 wt%. A slight increase in water absorption is observed at higher crosslinking concentrations.

In addition, a rise of water absorption capacity also results in increase swelling of graft copolymer that is unsuitable for a thickener. Figure 4.2 indicates the surface morphology of saponified starch-g-poly(acrylic acid) by varying the crosslinking concentrations at 0.5, 1.0, 1.5, 2.0, and 2.5 wt% based on the amount of monomer. SEM photographs illustrate the corresponding results in Table 4.1 and Figure 4.1. It seems that rising the crosslinking density increases the amount of porous polymer surfaces. The more porous surface polymer brings about a higher water adsorption capacity and swelling of the polymer. Figure 4.2 (a) shows the least porous surface of the graft copolymer prepared with 0.5 wt% crosslinking concentration, its water absorption is therefore the lowest. However, the amount of porous surface of graft copolymers in Figure 4.2 (b)-(c) is slightly different although the crosslinking concentration is higher. This can be attributed to decrease the size of mesh width

within the gels because of crosslinking reaction [45]. Consequently, their water absorption capacity increases insignificantly.

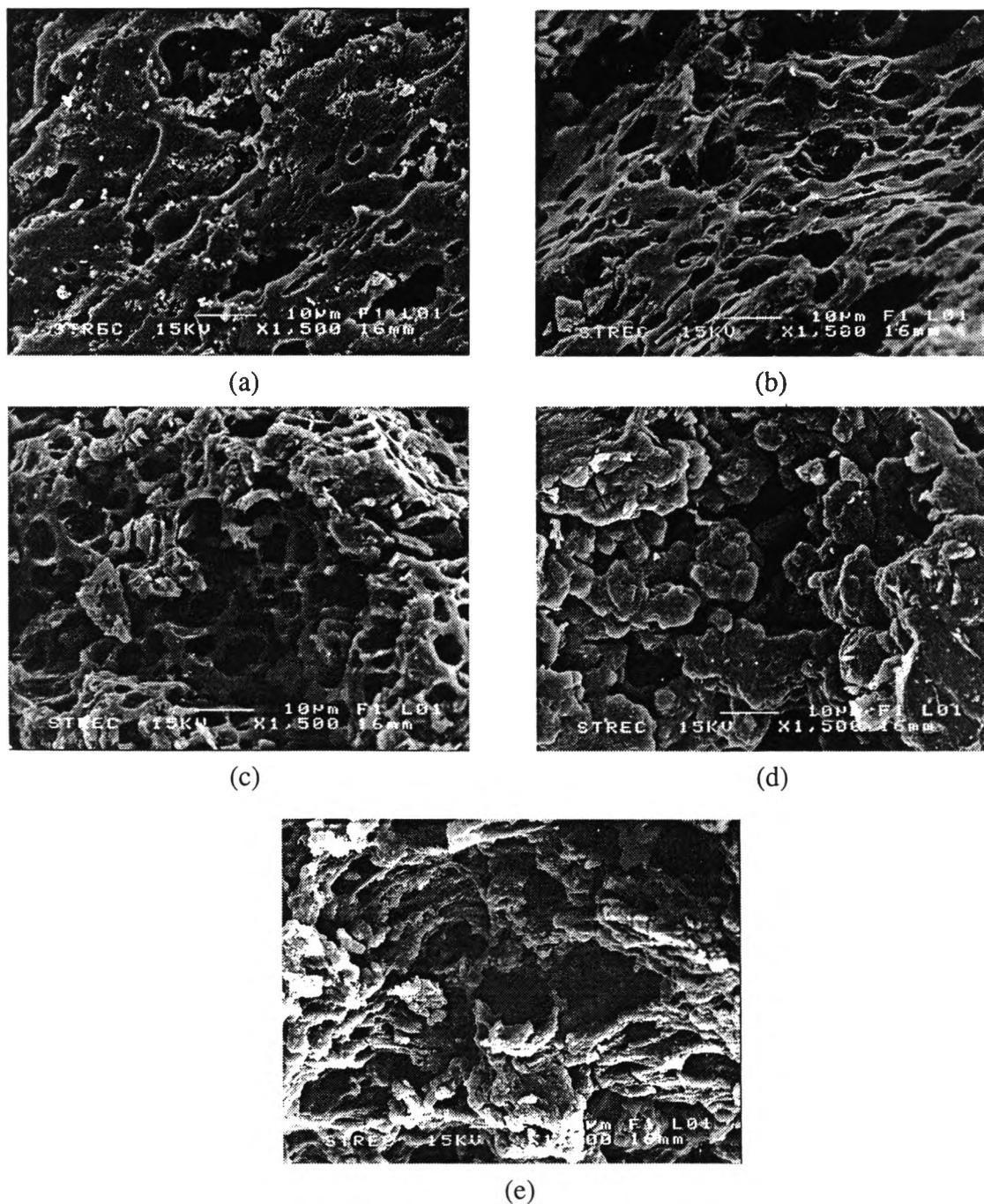


Figure 4.2 SEM photographs of the starch-g-poly(acrylic acid) prepared at different crosslinking concentrations: (a) 0.5, (b) 1.0, (c) 1.5, (d) 2.0, and (e) 2.5 wt% based on amount of monomer (x1500)

4.2 The Rheological Properties of Thickeners

The rheological properties of thickener were studied as a function of concentration (6, 8, 10, and 12 wt%) of saponified starch-g-poly(acrylic acid) in distilled water. The effect of crosslinking concentration on the rheology of thickeners was investigated.

The rheology profiles of thickeners with different crosslinking concentration at various shear rates are given in Table 4.2 and corresponding illustrations in Figures 4.3-4.11. It is found that the viscosity curves display a decrease in viscosity while the flow curves illustrate an increase in shear stress with an increase in shear rate. This property is known as shear thinning or pseudoplasticity. Shear thinning of the thickeners is believed to occur when the graft copolymer, which consist of the bundles of polymer chain, held together by the crosslinker are torn away by shearing force and dimensions of the packaged molecules therefore reduced [46].

For thickening agent, the gel is dispersed when water has been added, the visco-elasticity occurs when the swollen gel particles are in an intimate contact. If the mixture is diluted (low concentration) to a level at which the swollen gel particles are no longer in contact, being separated and then the mixture viscosity and elasticity decrease dramatically [2].

4.2.1 The Effect of Crosslinking Concentration on Rheology of Thickeners

Figures 4.3-4.6 show the effect of crosslinking concentration on viscosity and flow behavior of thickener solutions prepared using the different concentrations of starch graft copolymer. It is seen that for a given rate of shear, the viscosity of

Table 4.2 Rheological Behavior of Thickener Solutions with Various Crosslinking Concentrations at 25°C

Thickener Solution (wt% SPAA ^a)	Shear Rate (Sec ⁻¹)	Log Viscosity (Pa s) ^b					Log Shear Stress (N m ⁻²) ^b				
		Crosslinking Agent Concentration (wt%)					Crosslinking Agent Concentration (wt%)				
		0.5	1.0	1.5	2.0	2.5	0.5	1.0	1.5	2.0	2.5
6	1	0.70	0.88	0.92	1.18	1.35	0.70	0.88	0.92	1.18	1.35
	2	0.57	0.70	0.73	0.98	1.11	0.88	1.00	1.03	1.28	1.41
	4	0.32	0.49	0.55	0.78	0.90	0.92	1.10	1.15	1.38	1.50
	8	0.19	0.36	0.36	0.59	0.69	1.10	1.26	1.26	1.49	1.59
	20	-0.02	0.22	0.21	0.36	0.49	1.28	1.52	1.51	1.66	1.80
8	1	0.96	1.10	1.45	1.45	1.68	0.96	1.10	1.45	1.45	1.68
	2	0.80	0.94	1.20	1.30	1.45	1.10	1.24	1.50	1.60	1.75
	4	0.57	0.73	0.99	1.04	1.25	1.18	1.34	1.59	1.65	1.85
	8	0.40	0.60	0.75	0.88	1.06	1.30	1.50	1.65	1.78	1.97
	20	0.20	0.41	0.53	0.66	0.79	1.50	1.71	1.83	1.96	2.09
10	1	1.30	1.35	1.57	1.62	1.69	1.30	1.35	1.57	1.62	1.69
	2	1.11	1.19	1.34	1.42	1.48	1.41	1.49	1.64	1.72	1.78
	4	0.91	1.00	1.14	1.23	1.28	1.51	1.60	1.74	1.83	1.88
	8	0.70	0.85	0.95	1.04	1.08	1.60	1.75	1.86	1.95	1.98
	20	0.49	0.64	0.69	0.85	0.88	1.80	1.94	1.99	2.15	2.18
12	1	1.40	1.56	1.79	1.77	1.88	1.40	1.56	1.79	1.77	1.88
	2	1.21	1.39	1.57	1.57	1.66	1.51	1.69	1.87	1.87	1.96
	4	1.01	1.19	1.35	1.36	1.46	1.61	1.79	1.95	1.97	2.06
	8	0.83	1.02	1.14	1.17	1.26	1.73	1.92	2.04	2.08	2.17
	20	0.64	0.83	0.91	1.01	1.01	1.94	2.13	2.21	2.31	2.31

^aSPAA: Saponified Starch-g-Poly(acrylic acid)

^bSee Appendix A

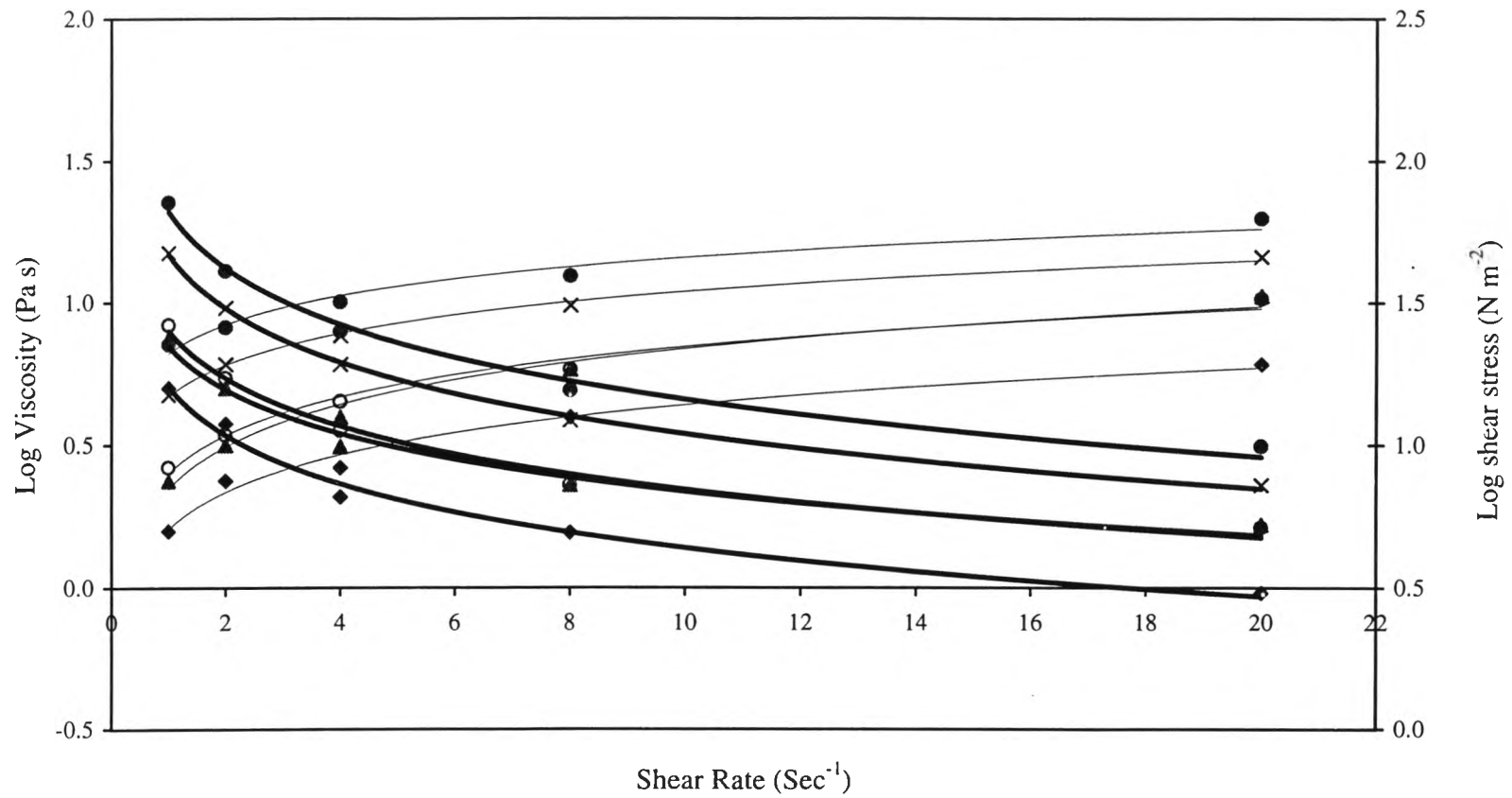


Figure 4.3 Effect of crosslinking concentration on viscosity and flow behavior of 6 wt% thickener solution

(◆ 0.5, ▲ 1.0, ○ 1.5, × 2.0, ● 2.5 Wt% crosslinking concentration, and ——— Flow curve, ——— Viscosity curve)

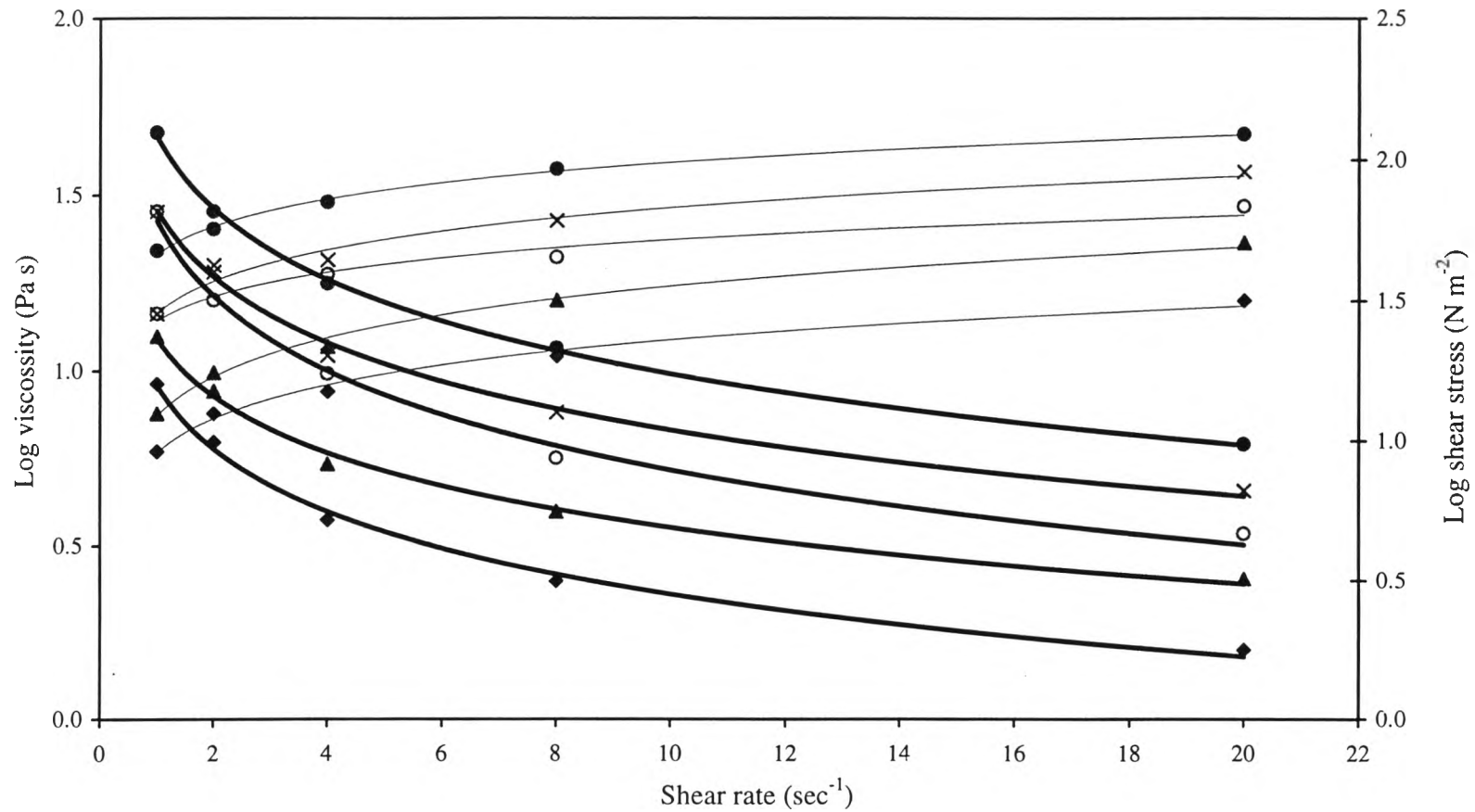


Figure 4.4 Effect of crosslinking concentration on viscosity and flow behavior of 8 wt% thickener solution

(◆ 0.5, ▲ 1.0, ○ 1.5, × 2.0, ● 2.5 wt% crosslinking concentration, and — Flow curve, — Viscosity curve)

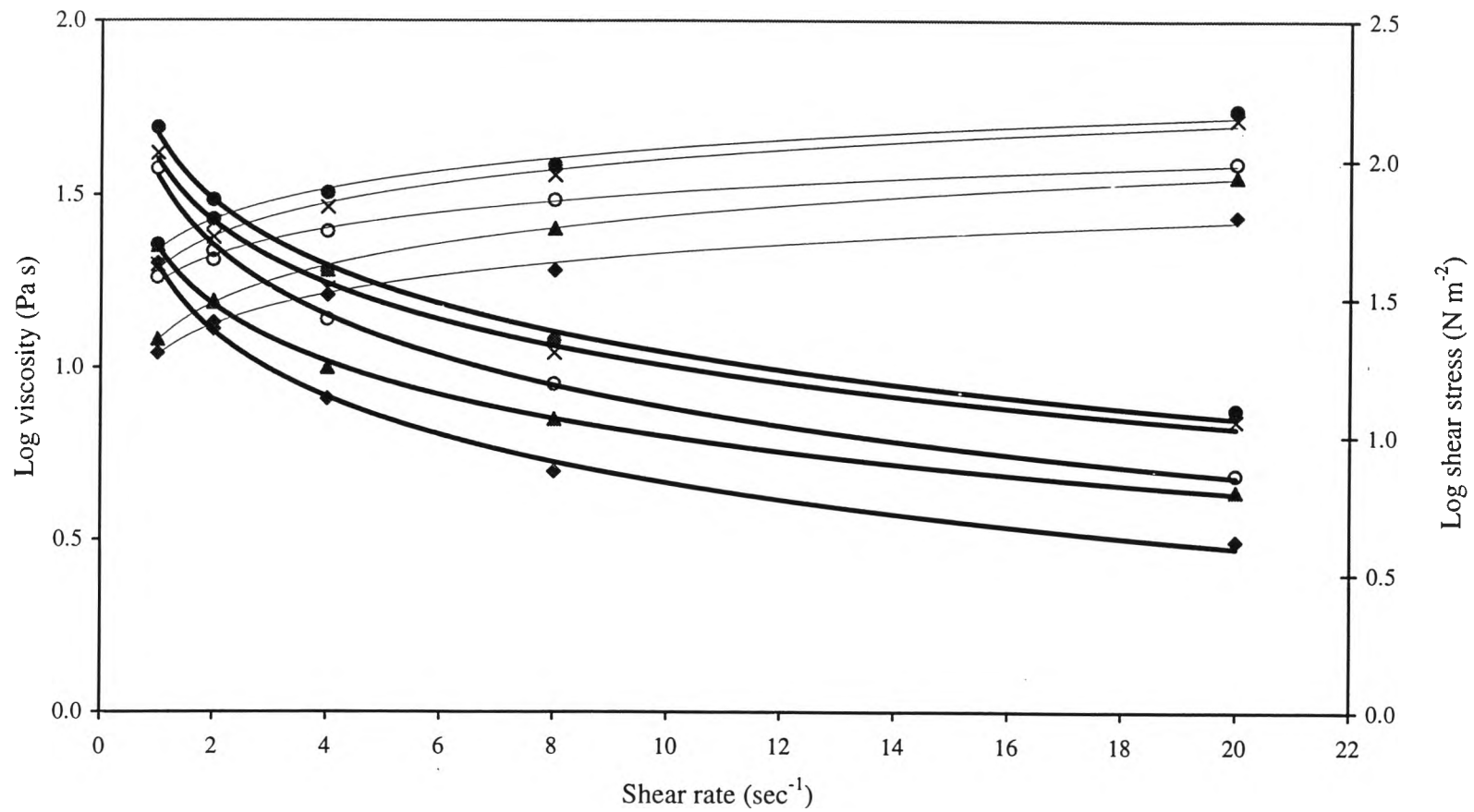


Figure 4.5 Effect of crosslinking concentration on viscosity and flow behavior 10 wt% thickener solution

(◆ 0.5, ▲ 1.0, ○ 1.5, × 2.0, ● 2.5 wt% crosslinking concentration, and — Flow curve, — Viscosity curve)

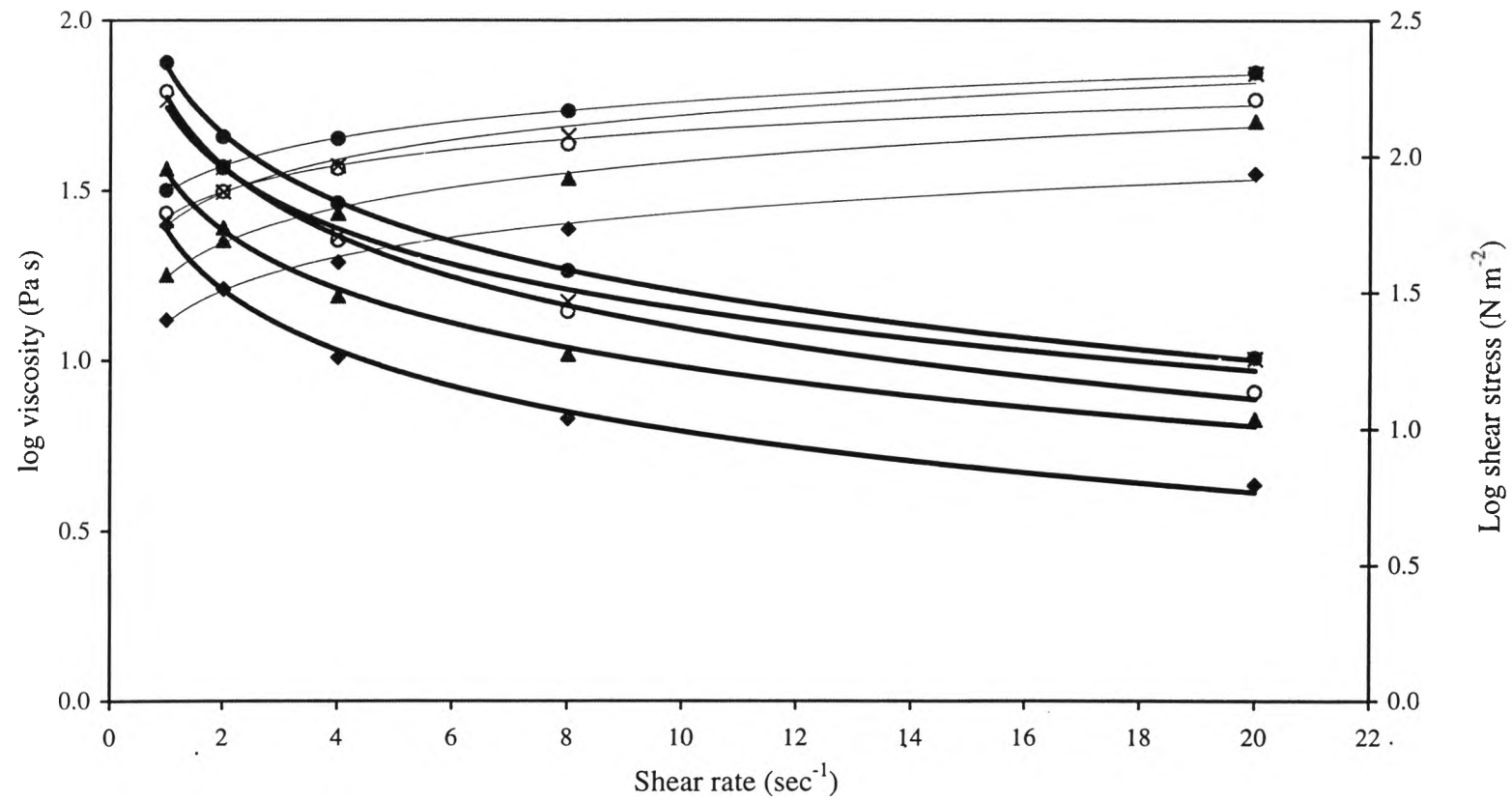


Figure 4.6 Effect of crosslinking concentration on viscosity and flow behavior of 12 wt% thickener solution

(◆ 0.5, ▲ 1.0, ○ 1.5, × 2.0, ● 2.5 wt% crosslinking concentration, and — Flow curve, — Viscosity curve)

thickener is increased and shear stress is also increased with a rise of the crosslinking concentration. Due to the fact that increasing the crosslinking entanglement point, higher shearing stress is clearly able to overcome the bonding forces and separate the polymer chain [45, 46]. The flow of thickener therefore takes place.

In addition, the characteristic of thickener solution prepared using 0.5 wt% crosslinking concentration gives homogeneous paste. On the other hand, the characteristic of the others using higher crosslinking agent concentration (1.0, 1.5, 2.0 and 2.5 wt%) give inhomogeneous pastes because of the great number of swollen molecular bundles and microaggregation of crosslinker. Although the thickener prepared with high crosslinking concentration give a high viscosity paste, it is not suitable for water-based inks due to more shear stress being required for the flow.

4.2.2 The Effect of SPAA Concentration on Rheology of the Thickeners

The effect of starch-g-poly(acrylic acid) concentration on the viscosity and flow behavior of thickeners is revealed in Figures 4.7-4.11. In every shear rate, increasing concentration of SPAA leads to increase of shear stress and viscosity of the thickener, as a result of the predominant influence of the gel fraction present.

The concentration of thickening agent often has a significant effect on the characteristics of the paste flow, more energy being required to separate and untangle the polymer chains in the more concentrated solutions [46].

Starch-g-poly(acrylic acid) synthesized with 0.5 wt% *N,N*-MBA crosslinking agent gave the minimum water absorption capacity and gave a suitable paste for screen printing. Therefore, it was selected to use as the thickener for water-based screen inks. However, the product would be used at 15 wt% or more in order to

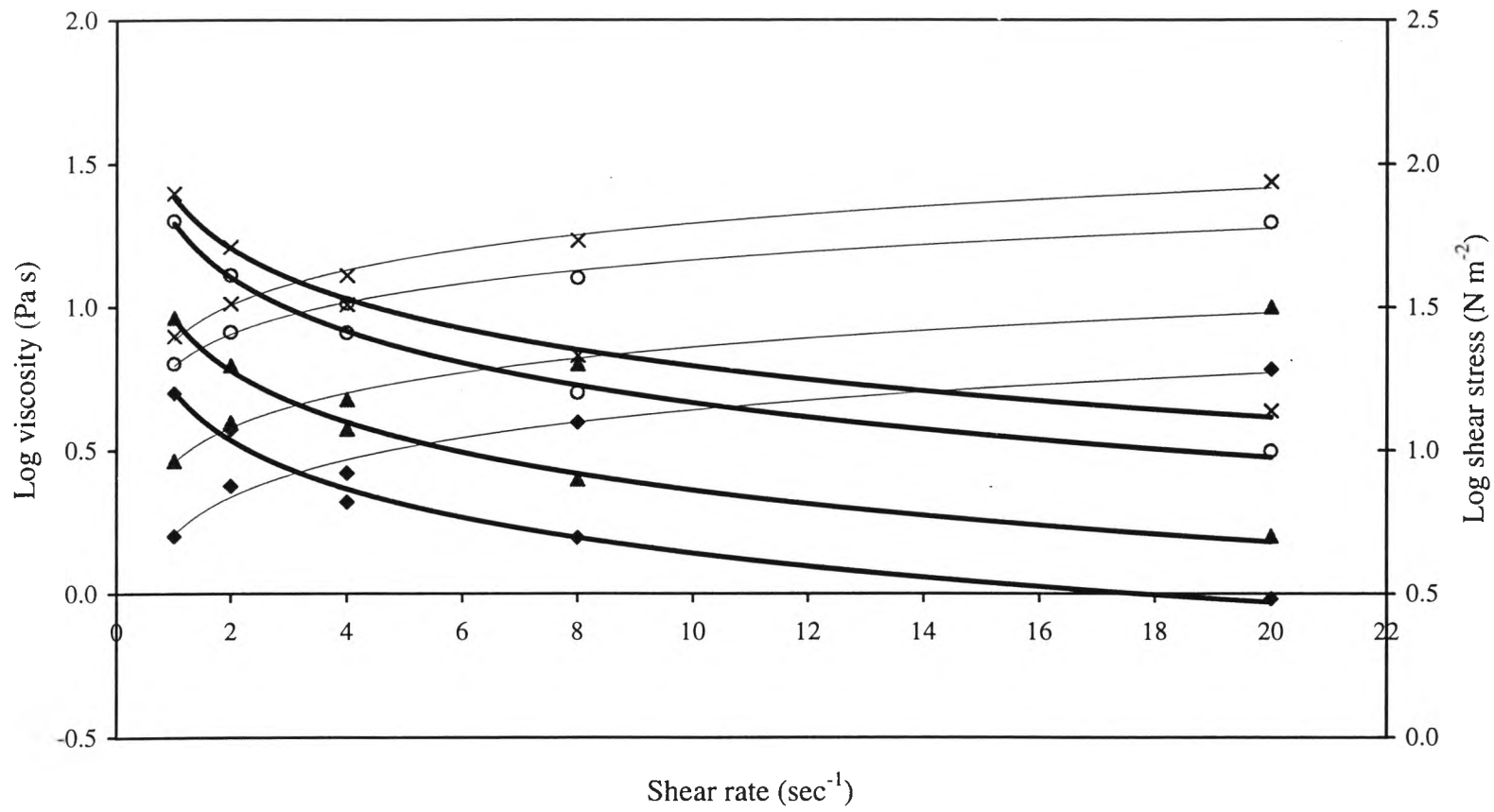


Figure 4.7 Effect of wt% SPAA content on viscosity and flow behavior of thickener with 0.5 wt% crosslinking

(◆ 6, ▲ 8, ○ 10, × 12 wt% SPAA content, and — Flow curve, — Viscosity curve)

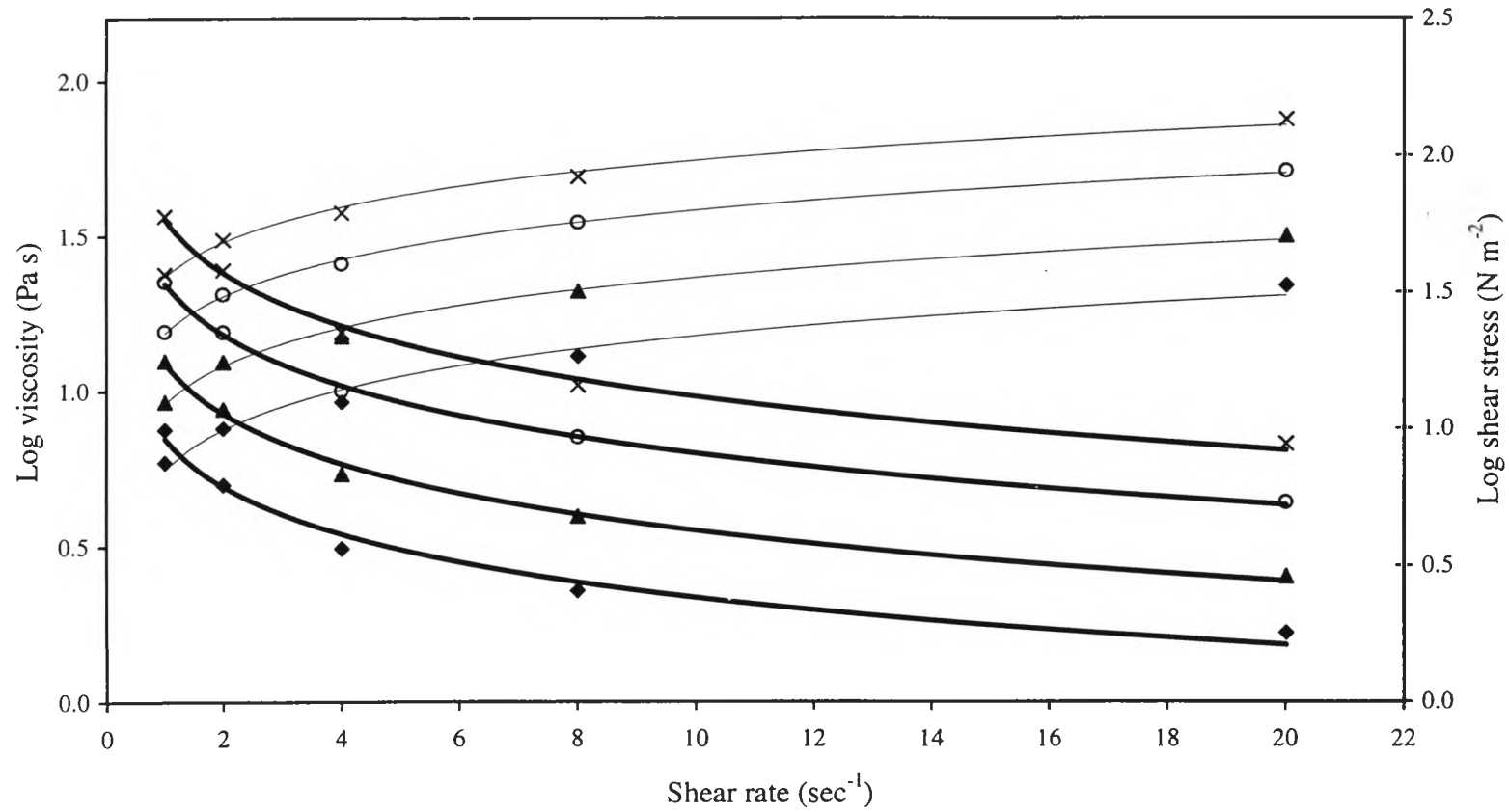


Figure 4.8 Effect of wt% SPAA content on viscosity and flow behavior of thickener with 1.0 wt% crosslinking

(◆ 6, ▲ 8, ○ 10, × 12 wt% SPAA content, and — Flow curve, — Viscosity curve)

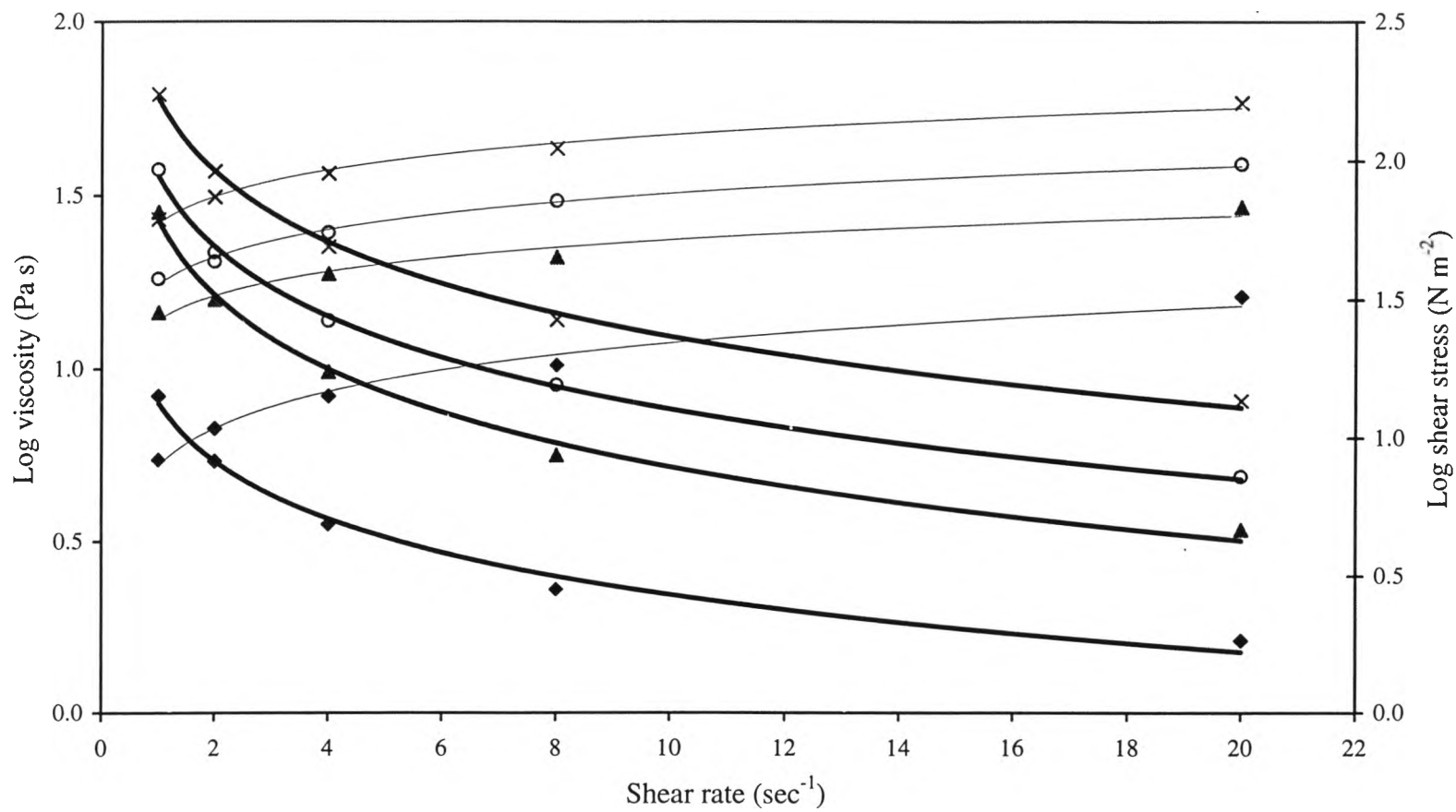


Figure 4.9 Effect of wt% SPAA content on viscosity and flow behavior of thickener with 1.5 wt% crosslinking

(\blacklozenge 6, \blacktriangle 8, \circ 10, \times 12 wt% SPAA content, and — Flow curve, — Viscosity curve)

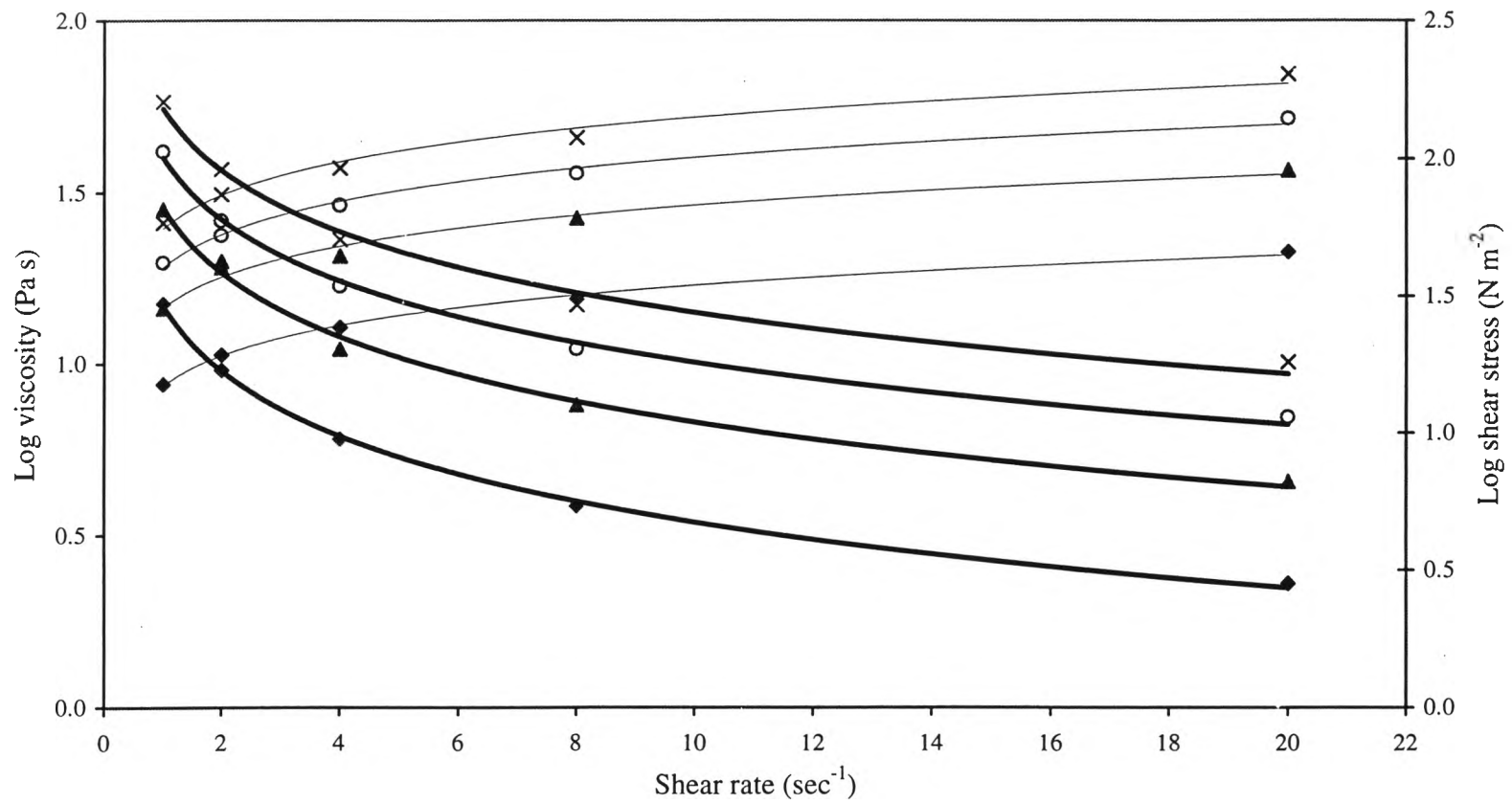


Figure 4.10 Effect of wt% SPAA content on viscosity and flow behavior of thickener with 2.0 wt% crosslinking
 (◆ 6, ▲ 8, ○ 10, × 12 wt% SPAA content, and — Flow curve, — Viscosity curve)

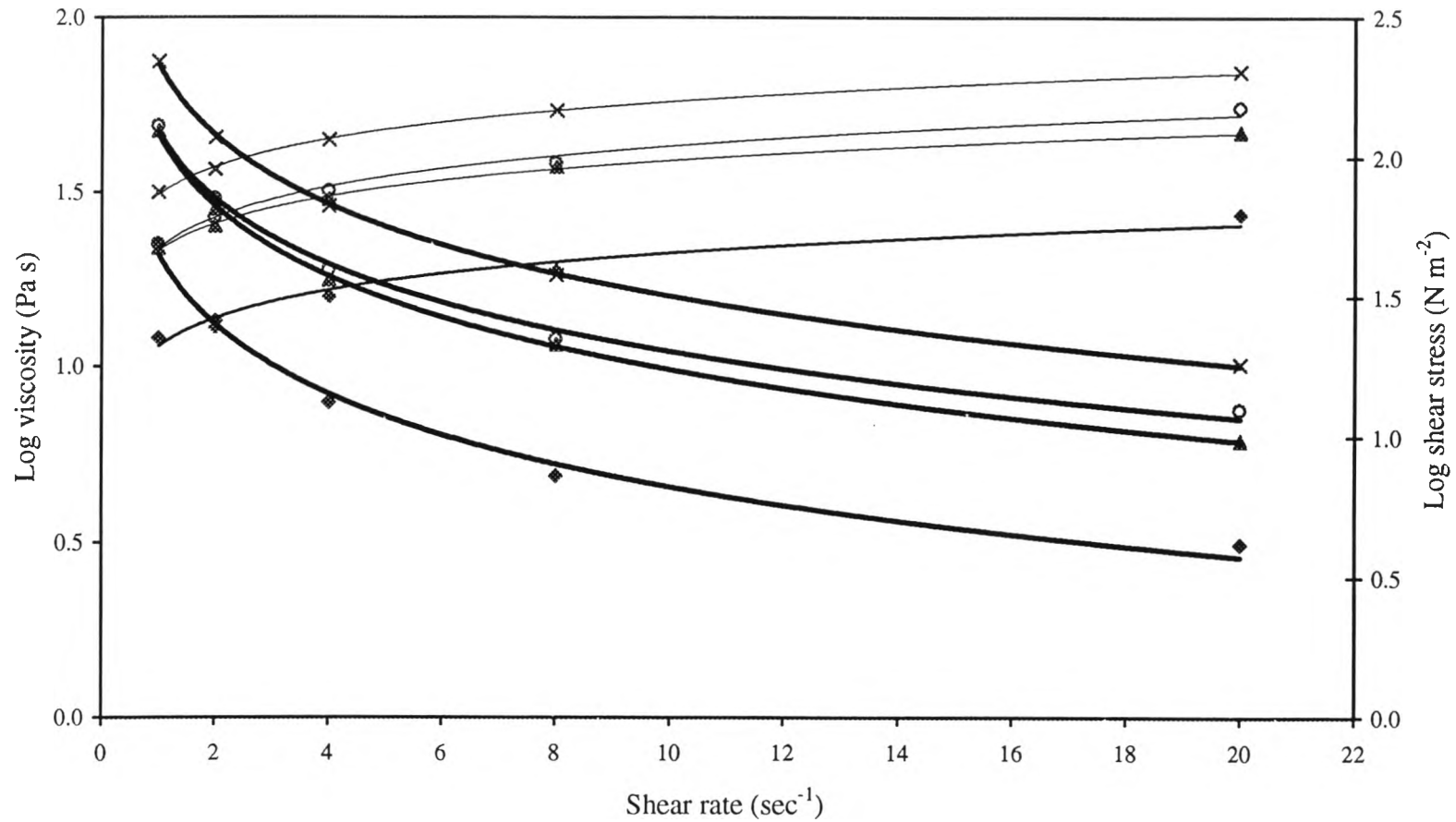


Figure 4.11 Effect of wt% SPAA content on viscosity and flow behavior of thickener with 2.5 wt% crosslinking

(◆ 6, ▲ 8, ○ 10, × 12 wt% SPAA content, and — Flow curve, — Viscosity curve)

obtain the desired higher viscosity. The viscosity and flow characteristic of this starch graft copolymer were studied prior to use. Table 4.3 and Figure 4.12 show rheological properties of 15 wt% thickener solution prepared by 0.5 wt% crosslinking agent. The viscosity and flow characteristic of this thickener display pseudoplasticity similar to other thickeners. It is a homogeneous and short flow paste, which is a stringent requirement for screen printing inks..

Table 4.3 Rheology Behavior of 15 Wt% Thickener Solution Prepared by 0.5 Wt% Crosslinking Agent Measured at 25°C

Shear Rate (sec ⁻¹)	Log Viscosity (Pa s) ^a	Log Shear Stress (N m ⁻²) ^a
	at 25 °C	at 25 °C
1	1.51	1.51
2	1.27	1.57
4	1.10	1.70
8	0.91	1.81
20	0.70	2.00

^aSee Appendix A

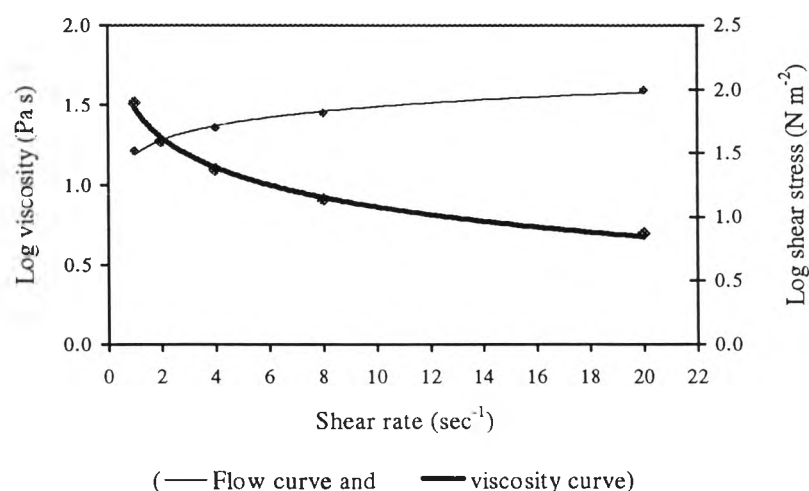


Figure 4.12 Viscosity and flow characteristics of 15 wt% thickener solution prepared by 0.5 wt% crosslinking agent measured at 25°C

4.3 Properties of the Prepared Water-Based Screen Inks

The two water-based screen inks were prepared using the thickener prepared with 0.5 wt% crosslinking agent. A 15 wt% solution of this thickener was used. The ink formulations are showed in Table 3.3. The properties of the inks were measured and the results obtained are presented as follows:

4.3.1 Viscosity and Flow Behavior of the Water-Based Inks

Table 4.4 reveals the rheology profiles of the prepared water-based inks at 25°C and Figures 4.13-4.15 illustrate the rheology of the two inks.

Table 4.4 Rheology Behavior of the Prepared Water-Based Inks at 25°C

Shear Rate (sec ⁻¹)	Ink Formula I (with non-silicone defoamer)		Ink Formula II (with silicone defoamer)	
	Log Viscosity	Log Shear Stress	Log Viscosity	Log Shear Stress
	(Pa s)	(N m ⁻²)	(Pa s)	(N m ⁻²)
1	1.74	1.74	1.68	1.68
2	1.51	1.81	1.45	1.75
4	1.27	1.88	1.23	1.83
8	1.05	1.95	1.01	1.92
20	0.78	2.08	0.74	2.04

In a similar manner as discussed previously, both ink I and ink II are characterized as the non-newtonian pseudoplastic behavior, which can be observed from the viscosity and flow curve in Figures 4.13 and 4.14, respectively. The viscosity of ink I is slight higher than that of ink II. The two inks give short flow

characteristic and they are sensitive to forces applied during printing. From Figure 4.15, when the shear stress increases slightly, the viscosity of the two inks drop dramatically.

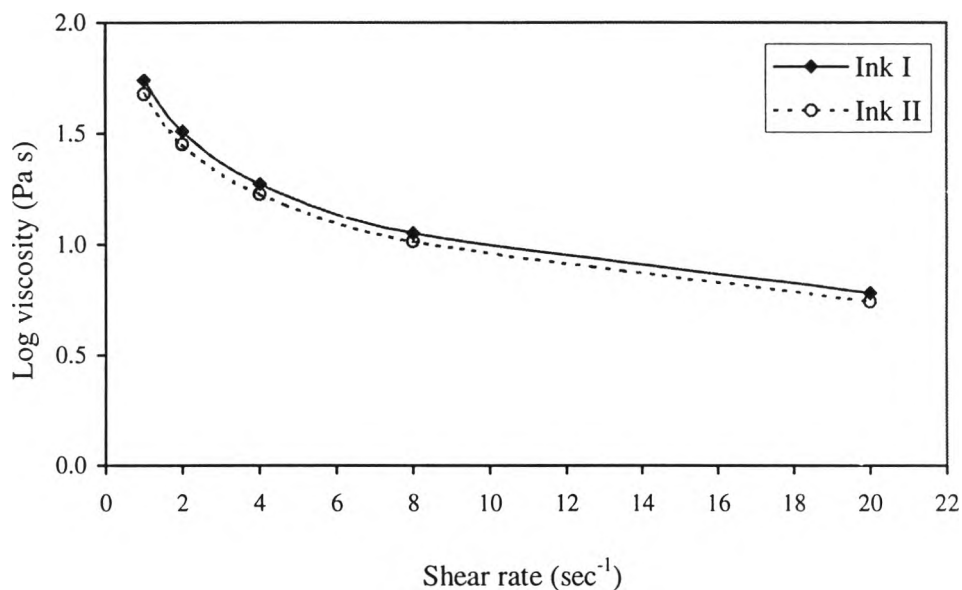


Figure 4.13 Viscosity the water-based inks at 25°C

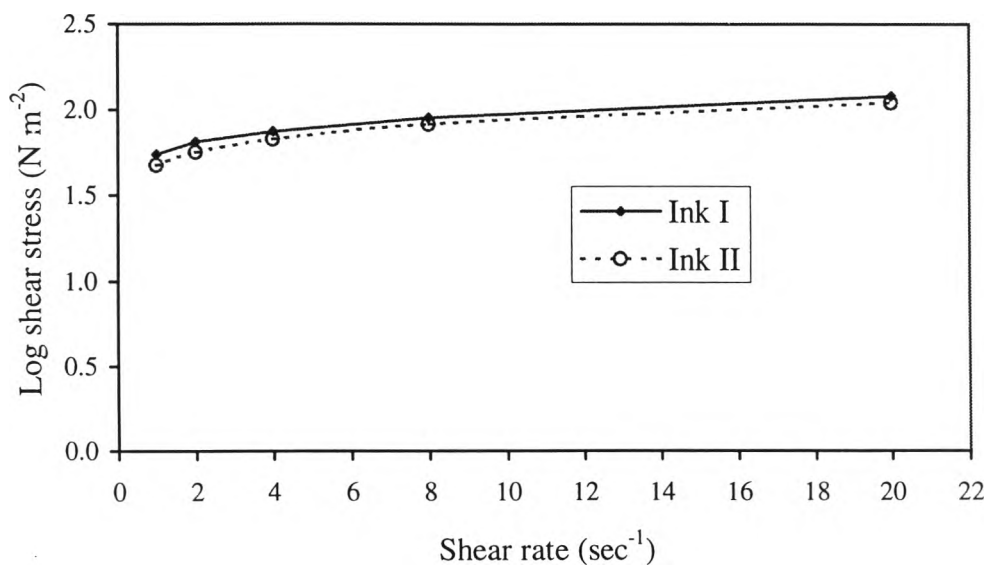


Figure 4.14 Flow characteristics of the water-based inks at 25°C

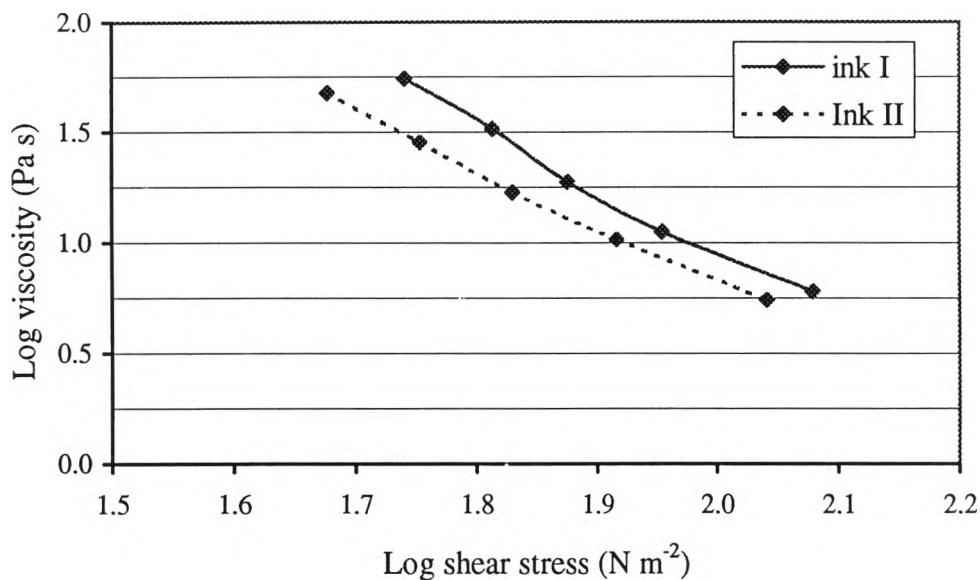


Figure 4.15 Shear stress and viscosity of the two water-based inks at 25°C

4.3.2 Dispersion (Fineness of Grind) of the Water-Based Inks

Fineness of grind of the prepared water-based inks were determined using a grind gauge. The results show that the ink I give degree of the fineness of grind at 22.5 μm size while the ink II shows 17.5 μm size on the grind gauge. So, the dispersion of the ink II is better than of the ink I.

To obtain a good dispersion process, three precautions must be controlled as follows [47]:

(a) We must remove the air or water on the crystal surface and replace it with the desired vehicle. This is called wetting.

(b) The pigment or particulates must be separated and uniformly distributed throughout the vehicle.

(c) The crystal surface of the pigment or particulate must be stabilized so that re-agglomeration or flocculation will not occur.

4.3.3 Surface Tension of the Water-Based Inks

Surface tensions of the two water-based inks are shown in Table 4.5 and Figures 4.16-4.17. The surface tension of ink I is 34 mN m^{-1} , while that of the ink II is about 32 mN m^{-1} . They are insignificant different because the same surfactant was used. However, the silicone defoamer used only for the ink II formulation also gives a low surface tension due to its nature of siloxane functionality. For the ink I, non-silicone defoamer was used.

For the surfactant, it is used to improve the wetting and spreading property but it induces foaming to the water-based inks. This problem could be solved by an addition of a defoaming agent, i.e. non-silicone and silicone defoamer.

We can determine the surface tension of the 100 wt% ink I and ink II are 34 and 32 mN m^{-1} , respectively.

Table 4.5 Surface Tension of Various Concentrations Water-Based Inks measured at 25°C

Concentration of Ink (wt%)	Surface Tension (mN m^{-1}) ^a	
	Ink Formula I	Ink Formula II
0 (distilled water)	72.1	72.1
0.1	42.8	45.2
0.5	42.6	39.3
1.0	39.7	36.8
10	34.8	30.8
15	34.8	30.6
20	34.4	32.0
25	33.9	32.3

^aSee Appendix B

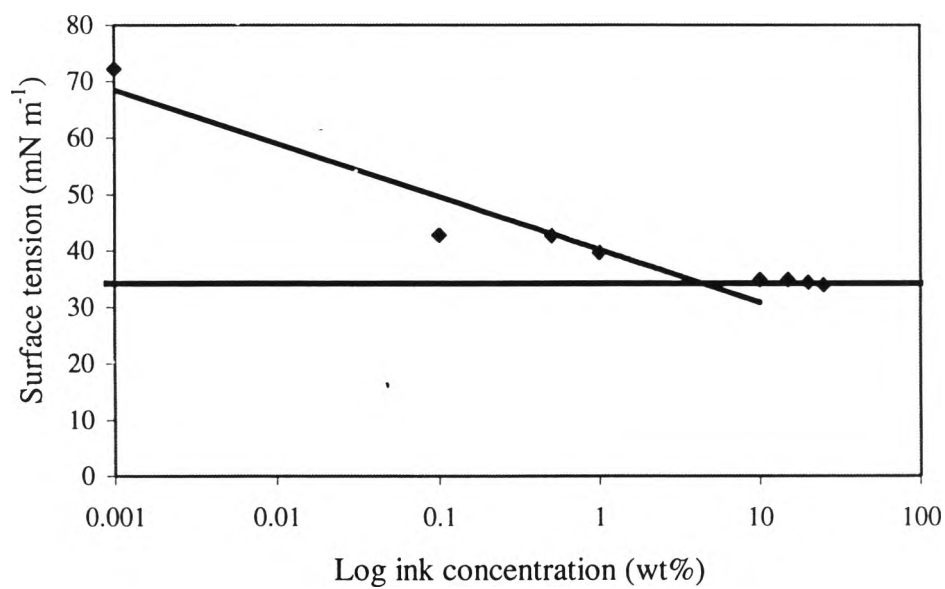


Figure 4.16 Surface tension of ink I

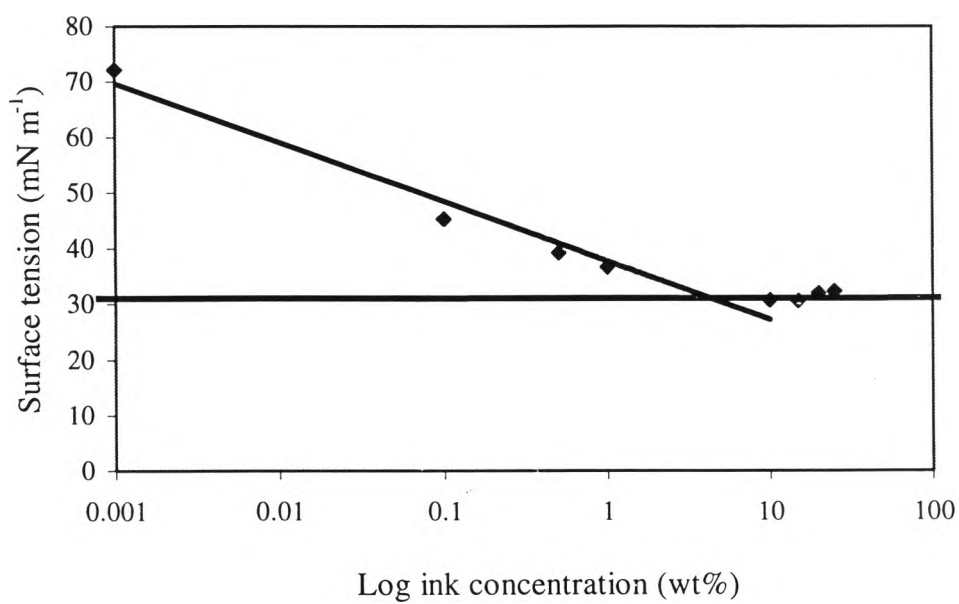


Figure 4.17 Surface tension of ink II

4.4 Surface Treatment

The purpose of corona treating is to remove the weak, low molecular weight contaminants that naturally occur on the surface of polyolefins [48]. Corona treatment increases the polar characteristics of the film surface. In most cases, the treatment is reversible and the rate of reversal is temperature and humidity dependent.

Corona is made up of pure electrical energy, or unpaired electron, and charged atoms and molecules representative of the local atmosphere. These electrons are known as free radical which are transitory high-energy entities that exists for only billionths of a second and are involved in all vinyl polymerization reactions. During corona treating, a mixture of activated oxygen species is present under the electrode. These species include free oxygen in its elemental form (O^*), ozone (O_3) and activated oxygen (O_2^*). Ultimately, these species act to increase molecular weight at the surface of the polymer film and at an oxidized surface layer.

The mechanism of corona treatment of film is based on consumption of oxygen generating surface polar functional group. Figure 4.18 illustrates the likely mechanism of corona treatment [49].

With water-based inks, corona treatment is important for the necessary ink wetting and effective drying speed. Polyethylene and polypropylene must be corona treated to at least 40 mN m^{-1} to assure proper ink wettability, adhesion, and drying rate [49].

The corona treated cast polypropylene (CPP) film was characterized in order to search for the optimum condition of treatment. The results obtained are discussed as follows.

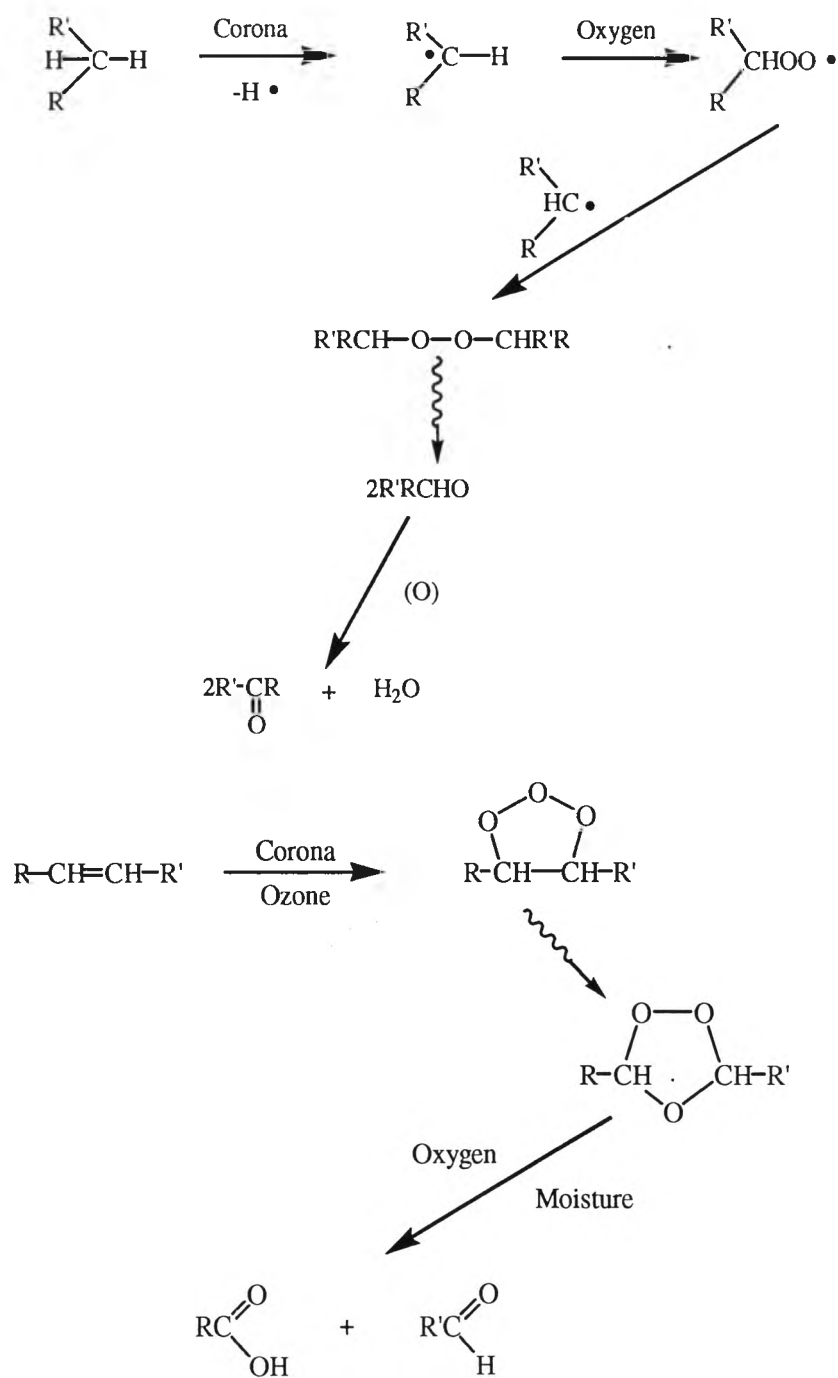


Figure 4.18 Probable mechanism of corona treatment

4.4.1 Surface Energy of Cast Polypropylene Film

4.4.1.1 Wetting Tension of Cast Polypropylene Film

Wetting tension of non-treated and treated plastic films was determined using the dyne solution test and contact angle measurement using methyl alcohol-water mixtures. The results are shown as follows:

(a) Dyne solution test

The effect of storage time on wetting tension of the treated plastic film is shown in Table 4.6. The results indicate that wetting tension of the treated plastic film decreases steadily with increase of storage time.

Table 4.6 Effect of Storage Time on Wetting Tension of CPP Film

Sample	Wetting Tension (mN m^{-1})		
	Storage Time (days)		
	0	7	14
Non-treated CPP film	Lower than 31		
300-watt treated CPP film	38	36	34
350-watt treated CPP film	42	39	36

(b) Measurement of contact angles of methyl alcohol-water mixtures on CPP film

Table 4.7 and Figure 4.19 illustrate the calibration curve plotted between the actual and measured surface tension. The surface tension values obtained from the calibration curve were utilized for determination of a critical surface energy of a plastic film by Zisman plot. These surface tension values are shown in Table 4.8.

Table 4.7 Actual and Measured Surface Tension Values of Methyl Alcohol-Water Mixtures at 20°C

Methyl Alcohol (Vol%)	Measured Surface Tension (mN m ⁻¹)	Actual Surface Tension (mN m ⁻¹)
0	73.0	72.8
10	60.8	59.0
25	51.2	46.4
50	39.2	35.3
60	37.6	33.0
80	31.2	27.3
90	27.6	25.4
100	24.9	22.7

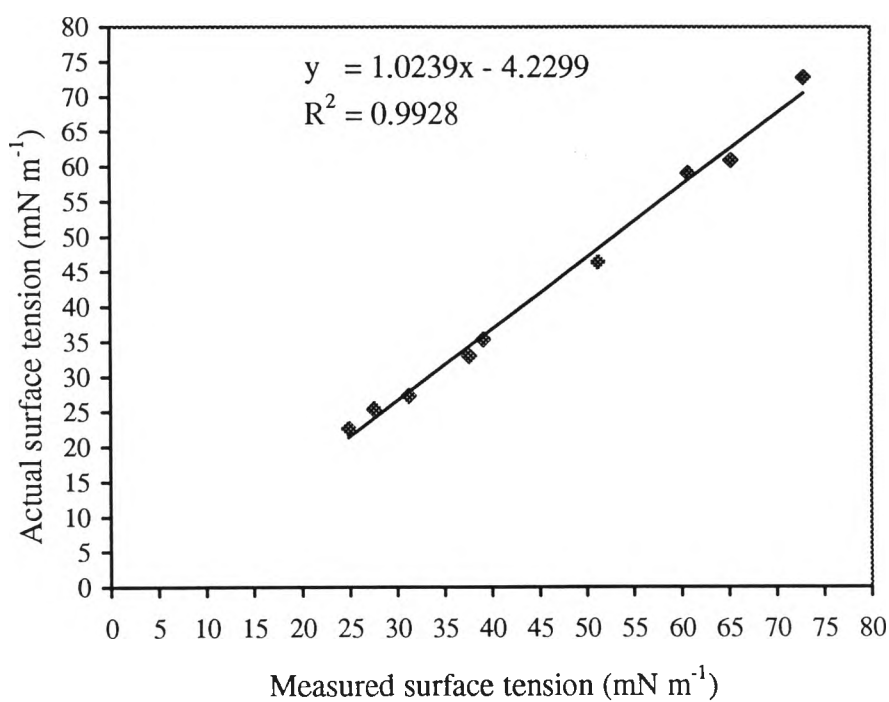


Figure 4.19 The calibration curve of surface tension of methyl alcohol-water mixtures at 20°C

Table 4.8 Calculated Surface Tension Values of Various Ratios of Methyl Alcohol-Water Mixtures at 20°C^a

Methyl Alcohol (vol %)	Surface Tension (mN m ⁻¹)
0	70.5
10	58.1
25	48.2
50	35.9
60	34.3
80	27.8
90	24.0
100	21.3

^aCalculation from the Calibration Curve: $y = 1.0239x - 4.2299$

Tables 4.9 and 4.10 show a correlation between the surface tension of various ratios of methyl alcohol-water mixture and the cosines of advancing and receding contact angles on the non-treated and treated plastic film with different storage times, respectively. The result shows that the cosines of the both advancing and receding contact angle increase with increasing the corona treatment. This indicates increasing corona treatment affects the surface energy of the substrate. Figures 4.20-4.22 illustrate the results similar to those of Tables 4.9 and 4.10. They demonstrate the difference between surface tension curves based on advancing and receding contact angle measurement, on non-treated, 300-watt, and 350-watt treated CPP films and storage time of 0, 7, and 14 days, respectively. The surface tension curves based on the receding contact angle is in higher position in the surface tension-contact angle diagram than the curves based upon the advancing contact angle measurement. The difference between two curves demonstrate the difference

Table 4.9 Surface Tension of Various Methyl Alcohol-Water Mixtures and Cosine of Advancing Contact Angle on Non-Treated and Treated CPP Films under Various Storage Times

Methyl Alcohol (vol%)	Surface Tension (mN m ⁻¹)	Cosθ (Advancing Contact Angle)												
		CPP Film												
		Non-Treated	Treating with 300 watts						Treating with 350 watts					
			Storage Time (days)						Storage Time (days)					
0	2	4	7	11	14	0	2	4	7	11	14			
0	70.48	0.05	0.36	0.26	0.28	0.22	0.22	0.19	0.50	0.42	0.39	0.38	0.35	0.34
10	58.07	0.14	0.39	0.38	0.33	0.30	0.32	0.29	0.55	0.50	0.45	0.44	0.47	0.46
25	48.23	0.23	0.54	0.43	0.46	0.44	0.46	0.45	0.59	0.53	0.54	0.52	0.51	0.50
50	35.86	0.36	0.71	0.64	0.64	0.53	0.64	0.58	0.76	0.77	0.75	0.73	0.75	0.71
60	34.3	0.47	0.81	0.65	0.64	0.64	0.65	0.65	0.84	0.80	0.78	0.76	0.79	0.80
80	27.75	0.64	0.90	0.82	0.79	0.77	0.80	0.79	0.96	0.93	0.87	0.88	0.87	0.90
90	23.99	0.73	0.95	0.90	0.89	0.81	0.86	0.85	1.00	1.00	1.00	1.00	1.00	0.99
100	21.28	0.77	1.00	1.00	0.95	0.95	0.95	0.94	1.00	1.00	1.00	1.00	1.00	1.00

Table 4.10 Surface Tension of Various Methyl Alcohol-Water Mixtures and Cosine of Receding Contact Angle on Non-Treated and Treated CPP Films under Various Storage Times

Methyl Alcohol (vol%)	Surface Tension (mN m ⁻¹)	Cosθ (Receding Contact Angle)												
		CPP Film												
		Non-Treated	Treating with 300 watts						Treating with 350 watts					
			Storage Time (days)						Storage Time (days)					
0	2	4	7	11	14	0	2	4	7	11	14			
0	70.48	0.17	0.59	0.45	0.52	0.48	0.50	0.34	0.79	0.69	0.79	0.72	0.73	0.73
10	58.07	0.28	0.68	0.55	0.58	0.66	0.61	0.56	0.80	0.77	0.80	0.77	0.77	0.76
25	48.23	0.36	0.80	0.67	0.71	0.75	0.69	0.69	0.80	0.78	0.77	0.79	0.81	0.81
50	35.86	0.54	0.84	0.80	0.80	0.72	0.73	0.81	0.87	0.88	0.88	0.88	0.91	0.90
60	34.3	0.60	0.91	0.83	0.82	0.79	0.85	0.83	0.92	0.89	0.87	0.88	0.91	0.91
80	27.75	0.81	0.95	0.90	0.90	0.88	0.89	0.91	1.00	0.99	0.97	0.98	0.96	0.98
90	23.99	0.89	0.99	0.99	0.97	0.93	0.94	0.95	1.00	1.00	1.00	1.00	1.00	1.00
100	21.28	0.95	1.00	1.00	1.00	1.00	1.00	1.00	1.00	1.00	1.00	1.00	1.00	1.00

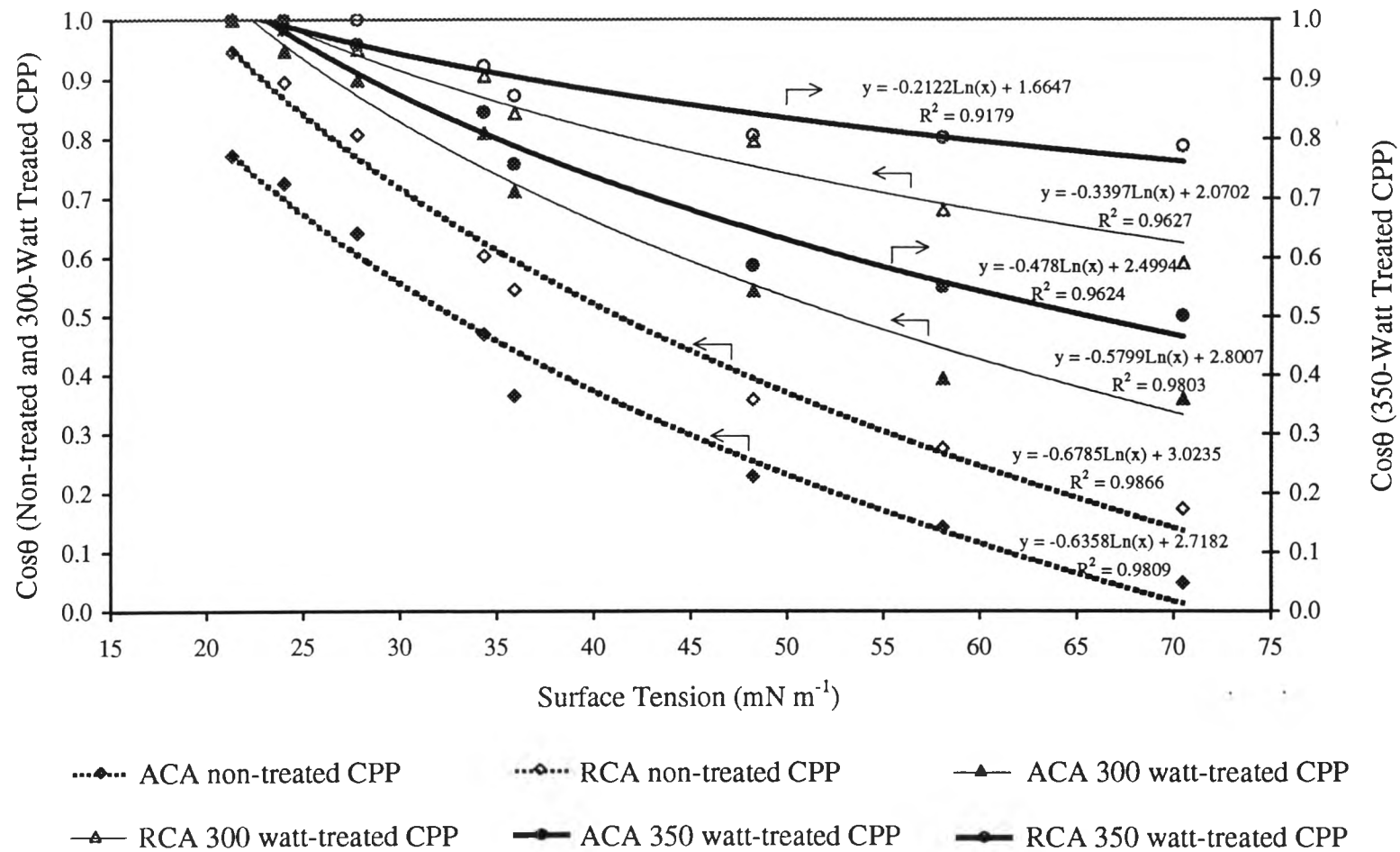


Figure 4.20 Effect of corona treatment of CPP films on advancing and receding contact angles measured with methanol-water mixtures

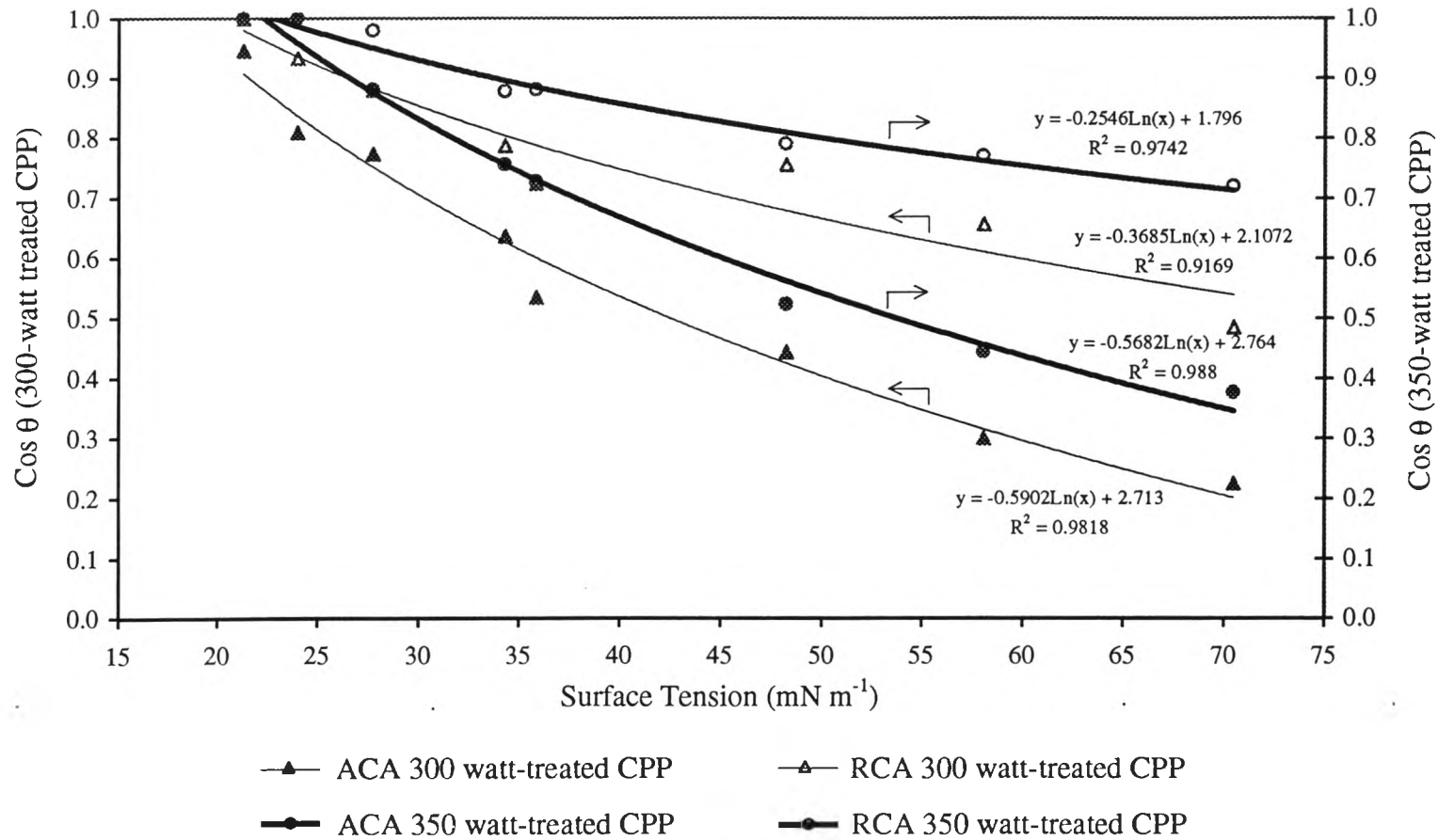


Figure 4.21 Effect of corona treatment of CPP films after seven days of storage time on advancing and receding contact angles measured with methanol-water mixtures

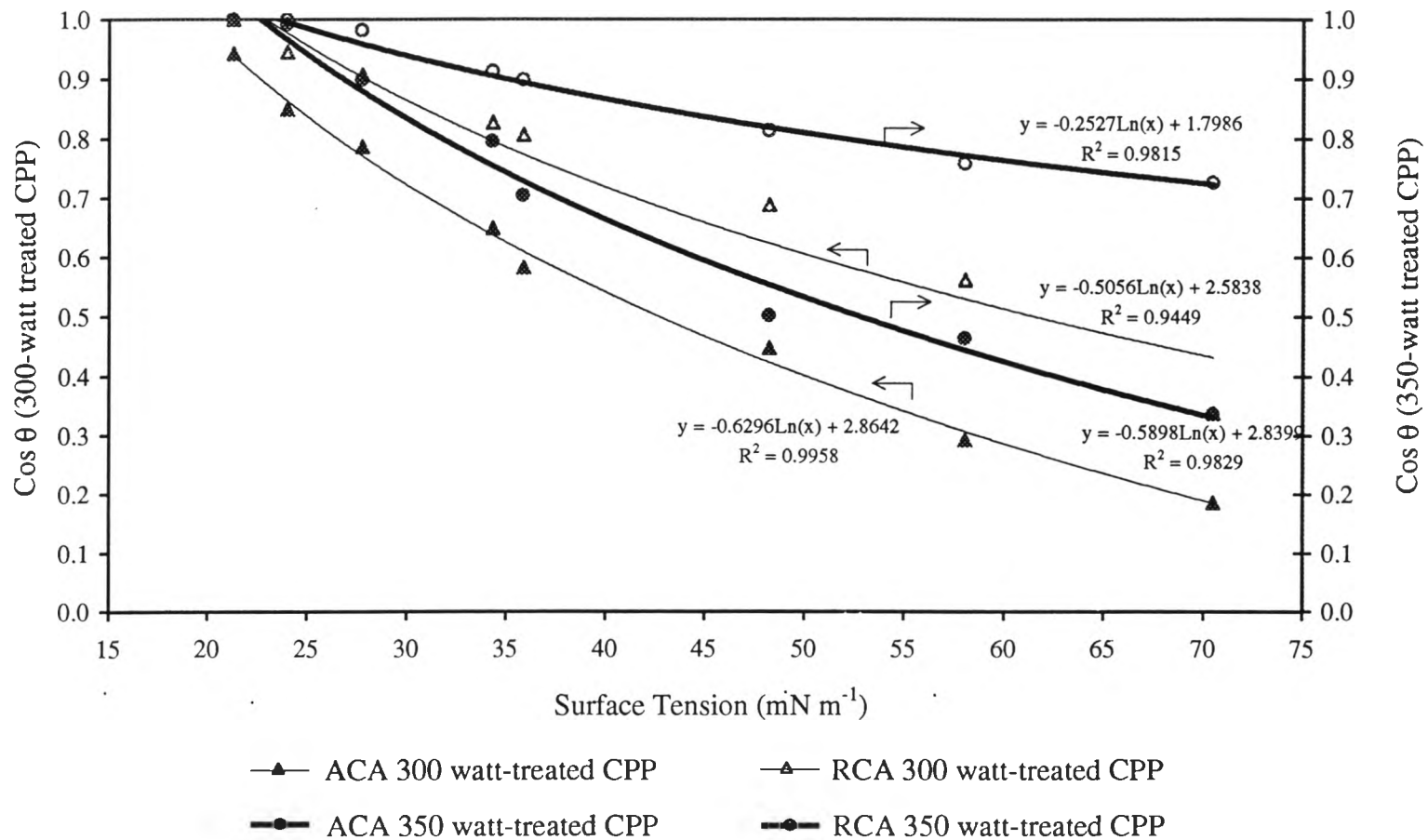


Figure 4.22 Effect of corona treatment of CPP films after fourteen days of storage time on advancing and receding contact angles measured with methanol-water mixtures

between the tendency of the liquid to spread and the contact. Approximately, the advancing contact angle illustrates the spreading of ink, i.e. printability and penetration into recessed areas, while the receding contact angle indicates the tendency of the ink to leave the substrate, i.e. adhesion for a solid density printed film. It can be seen that the gap between the two curves increases with increasing treatment of the plastic film. This indicates that adhesion may be improved by treatment of the plastic film, while printability may not be significantly improved [22].

We can determine critical surface energy of plastic film by solving the curve fitting equations (Least squared analysis) in Figures 4.20-4.22. The critical surface energy of the plastic film is shown in Table 4.11.

Table 4.11 Critical Surface Energy of the CPP Film in Terms of the Extent of Treatment and Storage Times.

Surface Tension Curve	Critical Surface Energy (mN m^{-1})		
	Storage Time (days)		
	After Treatment	7	14
ACA non-treated CPP	15	-	-
RCA non-treated CPP	20	-	-
ACA 300-watt treated CPP	22	18	19
RCA 300-watt treated CPP	23	20	23
ACA 350-watt treated CPP	23	22	23
RCA 350-watt treated CPP	23	23	24

From Table 4.11, The critical surface energy increases with increasing treatment watt. Nevertheless, the plastic films with treated 300 or 350 watts (output power) are insignificantly different, because an adequate energy interval used for

Table 4.12 Advancing and Receding Contact Angles of Methyl Alcohol-Water Mixtures on 300-Watt Treated CPP Film for Different Storage Times

Methyl Alcohol (vol%)	Surface Tension (mN m ⁻¹)	Advancing Contact Angle (degrees)						Receding Contact Angle (degrees)					
		Storage Time (days)						Storage Time					
		0	2	4	7	11	14	0	2	4	7	11	14
0	70.48	69	75	74	77	78	79	54	63	59	61	60	70
10	58.07	67	67	71	73	72	73	47	57	55	49	53	56
25	48.23	57	65	63	64	62	63	37	48	45	41	46	46
50	35.86	45	50	50	58	50	54	33	37	37	44	43	36
60	34.30	36	49	50	51	50	49	25	34	35	38	32	34
80	27.75	26	35	38	39	37	38	18	25	26	28	27	25
90	23.99	19	25	27	36	31	32	10	10	15	21	20	19
100	21.28	0	0	18	19	18	20	0	0	0	0	0	0

Table 4.13 Advancing and Receding Contact Angles of Methyl Alcohol-Water Mixtures on 350-Watt Treated CPP Film for Different Storage Times

Methyl Alcohol (vol %)	Surface Tension (mN m ⁻¹)	Advancing Contact Angle (degrees)						Receding Contact Angle (degrees)					
		Storage Time (days)						Storage Time (days)					
		0	2	4	7	11	14	0	2	4	7	11	14
0	70.48	60	65	67	68	70	70	38	47	43	44	43	43
10	58.07	57	60	63	64	62	62	37	40	36	40	39	41
25	48.23	54	58	57	58	59	60	36	38	40	38	36	36
50	35.86	41	40	41	43	41	45	29	29	28	28	25	26
60	34.30	32	36	39	41	38	37	23	27	30	29	24	24
80	27.75	17	22	30	28	30	26	0	8	13	12	16	11
90	23.99	0	0	0	0	0	8	0	0	0	0	0	0
100	21.28	0	0	0	0	0	0	0	0	0	0	0	0

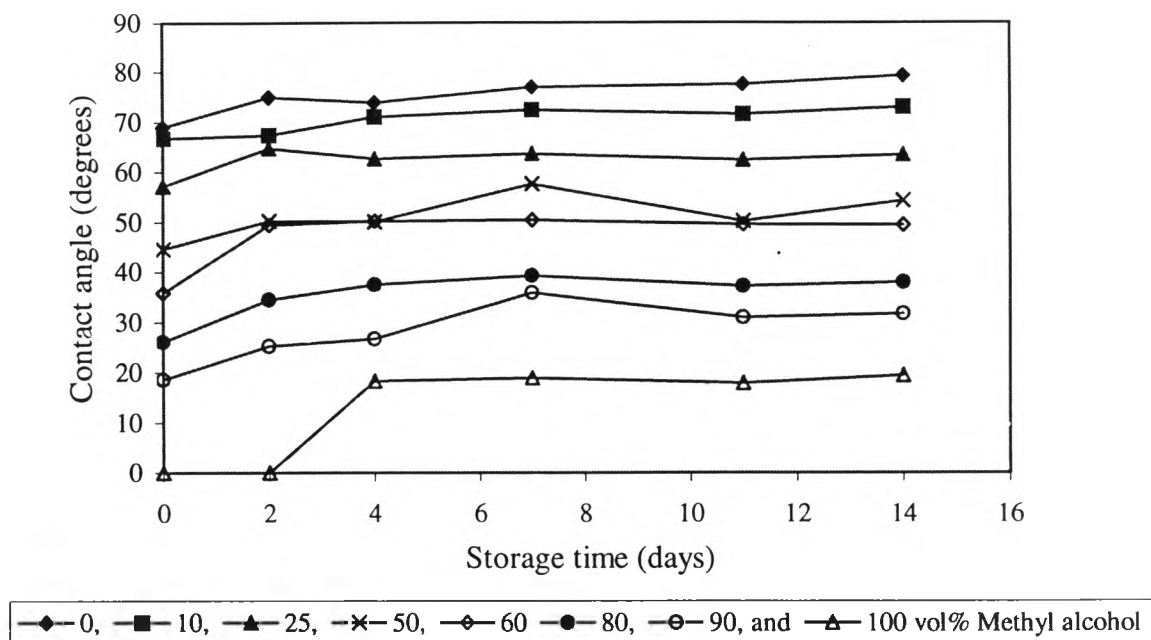


Figure 4.23 Effect of storage time on advancing contact angle of alcohol-water mixtures on the 300-watt treated CPP film

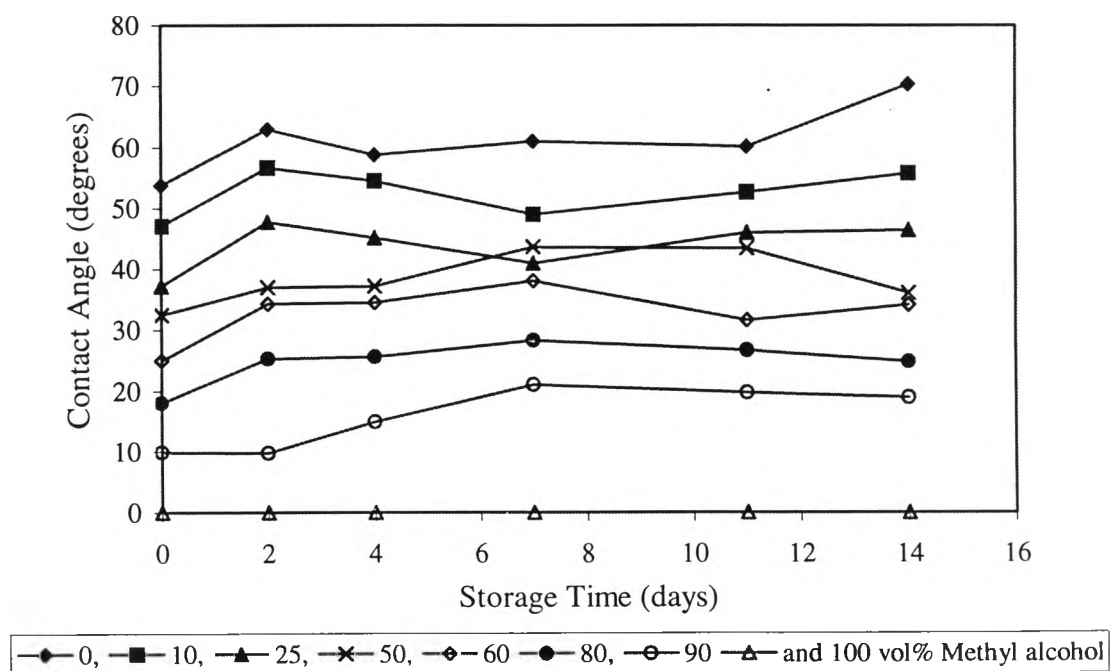


Figure 4.24 Effect of storage time on receding contact angle of alcohol-water mixtures on the 300-watt treated CPP film

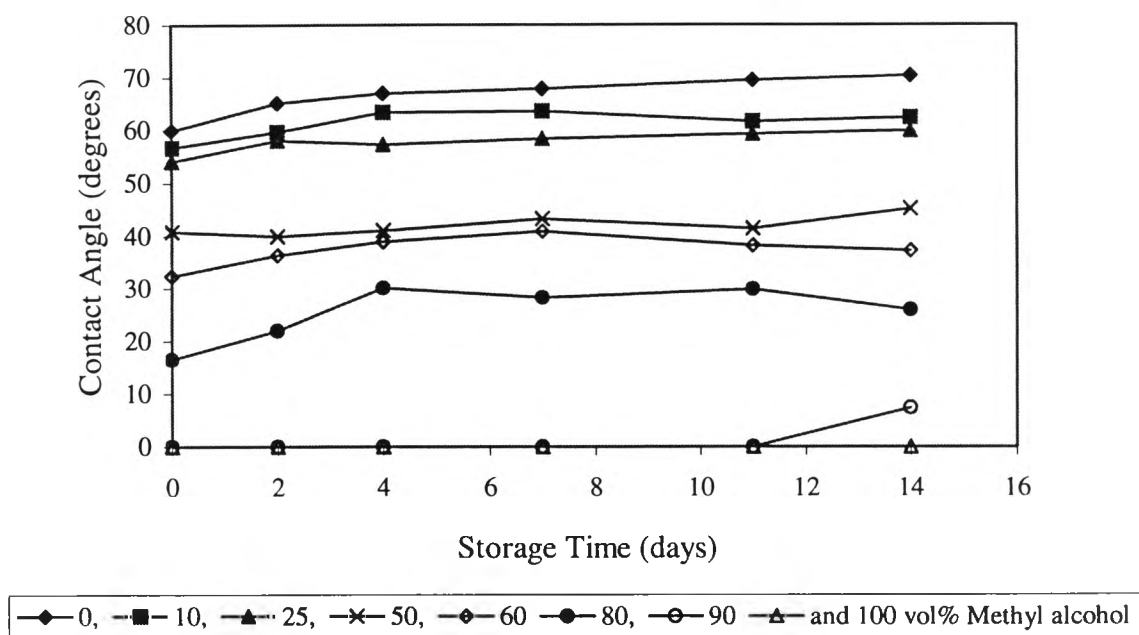


Figure 4.25 Effect of storage time on advancing contact angle of alcohol-water mixtures on the 350-watt treated CPP film

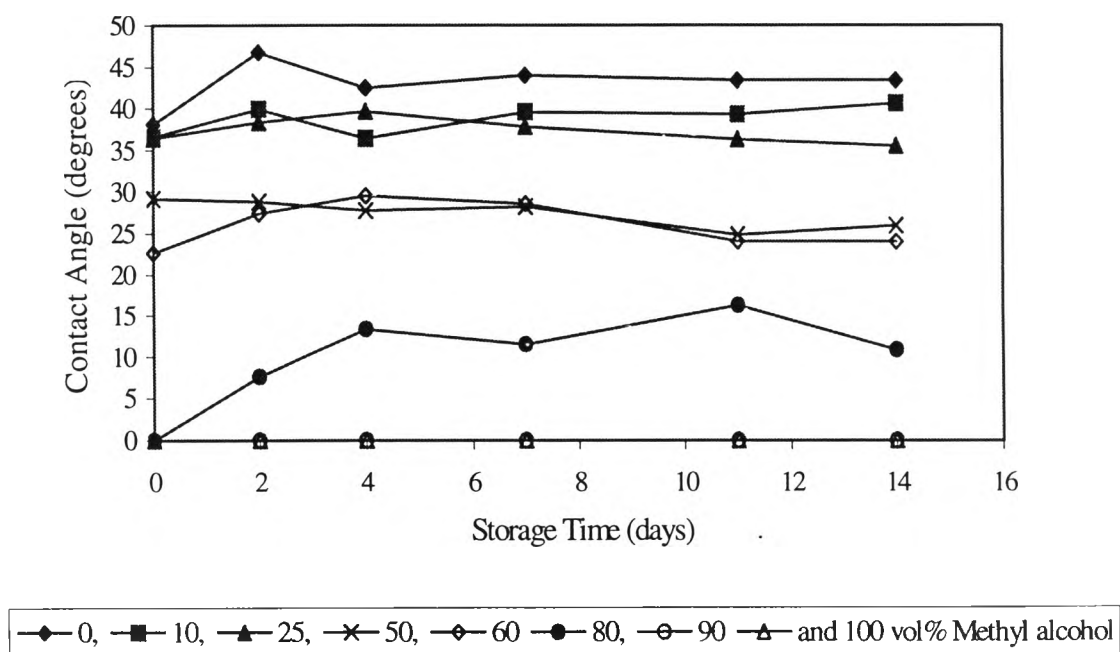


Figure 4.26 Effect of storage time on receding contact angle of alcohol-water mixtures on the 350-watt treated CPP film

enhanced treatment and the instability of the treatment. Besides, the length of storage time of the film slightly affects the film critical surface energy.

As for a requirement for a good printing on polyolefin plastic films, the critical surface energy of the substrate (film) must be at least equal to or at large greater than the surface tension of a printing ink [22]. That is, the highest surface tension of an ink must not be higher than 23 mN m^{-1} , which is equivalent to the critical surface energy of the plastic film treated with 350 watts (out put power). Wetting of substrate therefore takes place instantaneously and properly.

(c) The effect of storage time on contact angle of methyl alcohol-water mixture on treated CPP film

Tables 4.12-4.13 show the effect of film storage time on advancing and receding contact angles of alcohol-water mixtures (vol%) on the treated sample films and the corresponding results illustrated in Figures 4.23-4.26. When the storage time increases, both advancing and receding contact angles tend to increase. The contact angle increases significantly after storing the treated films for only 2 days. The contact angles then increase marginally and reach a stable stage after 4 days of storage. This indicates that the surface energy of treated plastic films decreases with increasing storage time.

4.4.1.2 Surface Energy Components of CPP Film

The polarity of surface, which is another important parameter is a prime key to properly interpreting surface energy data [29]. Table 4.14 shows the surface energy values calculated from the experimental data measured with water and 2-ethoxyethanol. For evaluating the surface energy, the polar and dispersive energy components for water are 50.2 and 22.6 mN m^{-1} , respectively, and those for 2-ethoxyethanol

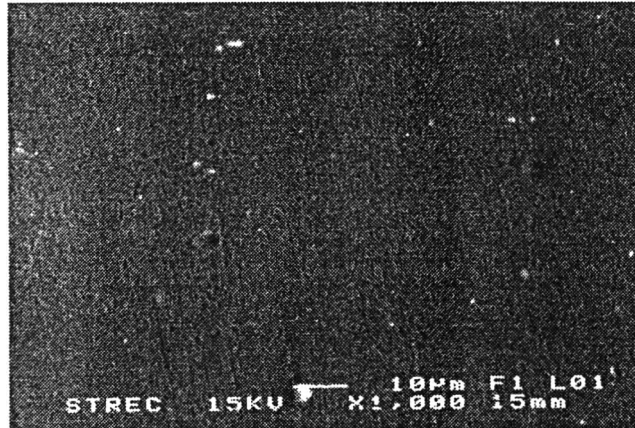
are 5.0 and 23.6 mN m⁻¹, respectively. It is inevitable from Table 4.14 that the polar surface energy is very low for the non-treated CPP film. Increasing the corona treatment on the CPP film increases the polar surface energy component rapidly while the dispersive surface energy component is not significantly different. For this experiment, the CPP film treated with 350 watts of energy has the highest polar surface energy. The polar surface energy is in the range 20-30 mN m⁻¹. In addition, the polar surface energy component decreases with increasing storage time. In order to well adhere the ink to the Cpp film, the polar and dispersive surface energy components of the formulated ink should be similar to those of the substrate [50].

Table 4.14 Surface Energy Components of the Non-Treated and Treated CPP Film with Various Levels of Treatment and Storage Times

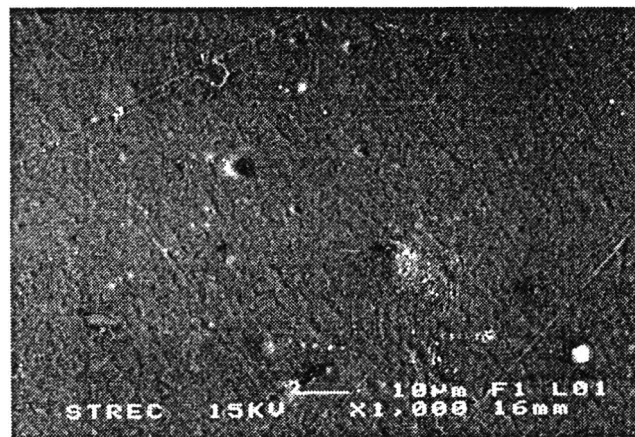
CPP with Treatment and Storage Time	Surface Energy (mN m ⁻¹)			% Polarity	Polar/Dispersive Ratio
	Total	Polar	Dispersive		
Non-treated	25.1	4.9	20.2	19.5	0.24
300-watt treated (0 day)	37.5	25.1	12.4	66.9	2.02
300-watt treated (7 days)	35.8	23.5	12.6	64.8	1.87
300-watt treated (14 days)	34.1	20.8	13.3	61.0	1.56
350-watt treated (0 day)	41.2	30.2	11.0	73.3	2.75
350-watt treated (7 days)	37.6	25.9	11.7	68.9	2.21
350-watt treated (14 days)	35.0	22.4	12.6	64.0	1.78

4.4.2 Surface Morphology of CPP Film

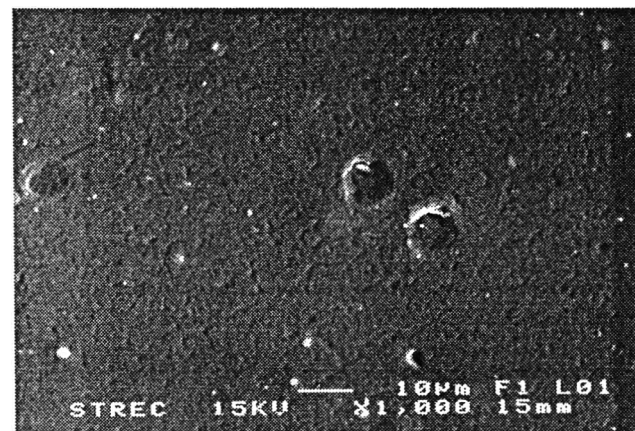
In addition to the surface chemistry measurement, the morphology of plastic film was characterized with scanning electron microscopy (SEM). The electron micrographs in Figure 4.27 demonstrate an increasing roughness of the film surface as



(a)



(b)



(c)

Figure 4.27 SEM photographs of CPP films with treatment energy levels of 300 and 350 watts: (a) non-treated, (b) 300-watt treated, and (c) 350-watt treated (x1000)

increasing treatment. The roughness at the 300 and 350-watt treated plastic films is slightly different. As high energy particles bombard the film being treated, small micro pits are formed. These are tiny holes dug by the charges [41]. Micropitting can lead to increased adhesion through mechanical keying and a greater potential bonding area. Unfortunately, it can also lead to reduced adhesion because a tiny area of bonding is achieved, or because stress concentration occurs due to the presence of voids.

It is well known in practice that the drop volume is increased, the apparent contact angle also increases, until maximum value is reached. This is called the advancing contact angle. Similarly, when the drop volume is decreased, the apparent contact angle decreases, until a minimum is reached. This minimum contact angle is the receding one. The phenomenon of having a different contact angle under advancing and receding condition is known as contact hysteresis [26, 27]. It is possible to find data on the advancing and receding contact angles measured by the sessile drop technique, simply putting a drop of liquid on the surface. This type of measurement is usually called static contact angles, as opposed to the dynamic contact angles, which are measured, for instance, by the tilting plate technique. This technique is a way of measuring both the advancing and receding contact angles, while the substrate is in motion.

Table 4.15 shows the advancing and receding contact angles obtained at various treatment levels. The contact angle hysteresis (a difference between the advancing and receding contact angle) increases with increasing level of treatment. This indicates an increase in surface roughness and heterogeneity [29]. Increasing the

corona treatment from 300 to 350 watts, slightly increases the hysteresis, due to the insignificant of the treatment level.

Table 4.15 Advancing and Receding Contact Angles on CPP Films

CPP Plastic Film	ACA ^a	RCA ^b	Hysteresis
Non-treated	89	80	9
300-watt treated	63	45	18
350-watt treated	60	40	20

^aACA: Advancing Contact Angle

^bRCA: Receding Contact Angle

4.5 Work of Adhesion of the Formulated Inks on Corona Treated CPP Plastic Films

When printing, besides the wettability of the surface required for images, sufficient adhesion of the printing ink film to the substrate is necessary [33]. From the results in Table 4.5, we can determine the surface tension of the two water-based inks (ink I and ink II). Since the surface tension values of ink I and ink II remain constant at 10 wt% concentration of the thickener. We used the ink concentrations of 10, 15, 20, and 25 wt% for the contact angle measurement in order to search for the adequate work of adhesion of the inks on the treated plastic films. Table 4.16 shows the contact angle of various concentrations of the ink I and ink II on the treated CPP film for different storage times. The results show the contact angles of the ink I and ink II on the treated films increase with increase the storage time. At every ink concentration and storage time, the contact angles of the ink I are lower than those of

the ink II. This indicates that the work of adhesion of the ink I is also higher than that of the ink II as shown in Table 4.17. Therefore, the ink I should well adhere to the treated films than should the ink II.

Table 4.16 Contact Angle of the Ink I and Ink II on the Treated Plastic Films for Different Storage Times

Ink Concentration (wt%)	Contact Angle (degrees)					
	Ink I			Ink II		
	Storage Time for Treated CPP (days)			Storage Time for Treated CPP (days)		
	0	7	14	0	7	14
10	18	20	22	23	25	25
15	19	19	23	21	25	27
20	18	21	22	22	24	24
25	19	21	23	23	25	24

Table 4.17 Work of Adhesion of the Ink I and Ink II on the Treated CPP for Various Storage Times

Ink Concentration (wt%)	Work of Adhesion (mN m^{-1})					
	Ink I			Ink II		
	Storage Time for Treated CPP (days)			Storage Time for Treated CPP (days)		
	0	7	14	0	7	14
10	68	68	67	59	59	59
15	68	68	67	59	58	58
20	67	67	66	62	61	61
25	66	66	65	62	62	62
Average of Work of Adhesion (mN m^{-1})	67	67	66	61	60	60

4.6 The Print Qualities of the Printed Plastic Film

The plastic films treated with 350 watts of output energy for 3 seconds have the optimum surface properties treatment for printing with the formulated water-based screen inks. The printed plastic films so obtained are illustrated in Figures 4.28-4.33.

The print qualities evaluation are given below:

a) % Dot Area and Dot Gain

Tables 4.18-4.19 show % dot area and dot gain of the plastic films printed by the ink I and corresponding results are illustrated in Figure 4.34. It is found that the unstorage plastic film printed by the ink I shows the highest dot gain (4 to 11%) at midtone area to 80% dot area while at the low % dot area and the shadow area of the print show some small percentage of dot loss. Because the ink I has low viscosity and high foaming property. For the plastic film printed by ink II, there are very high dot gain by 6-17% at 50 to 60 % dot area. Some dot loss (1 to 5%) was found at 10 % dot and solid area.

b) Tone Reproduction

Tone quality can be determined by measuring dot area (percentage of ink coverage on the substrate) with a transparent densitometer. From Table 4.20-4.21 and Figure 4.35, tone reproduction of the both plastic films printed by ink I and ink II are shown similarly. They are insignificant difference. Densities of the print at 0 to 90% dot area were reproduced similarly to the densities of the original film, while the density at solid tone so produced is dramatically different from that of the original film.

Screen 30 lpi

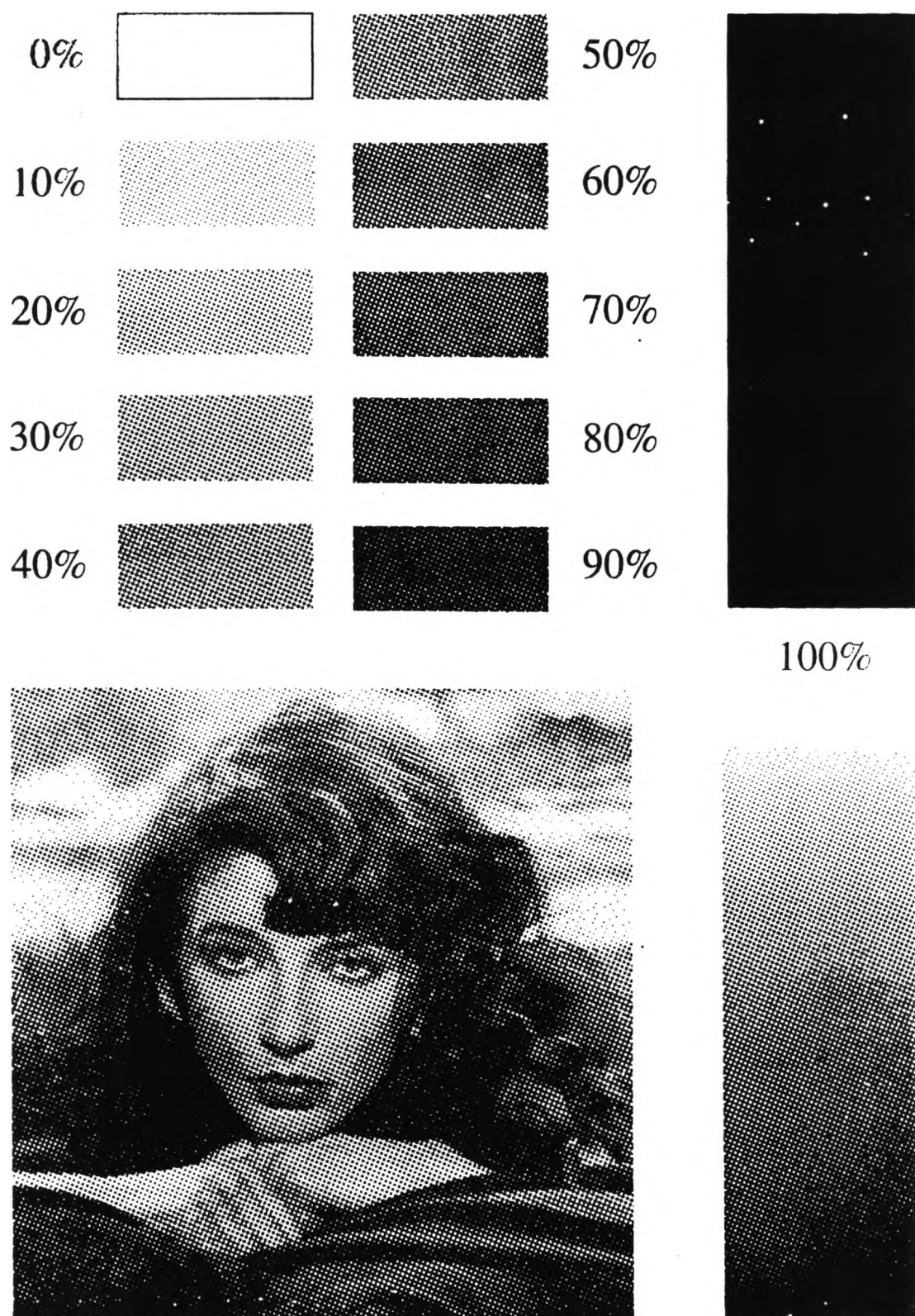


Figure 4.28 Printed image on the freshly treated CPP film printed with the ink I

Screen 30 lpi

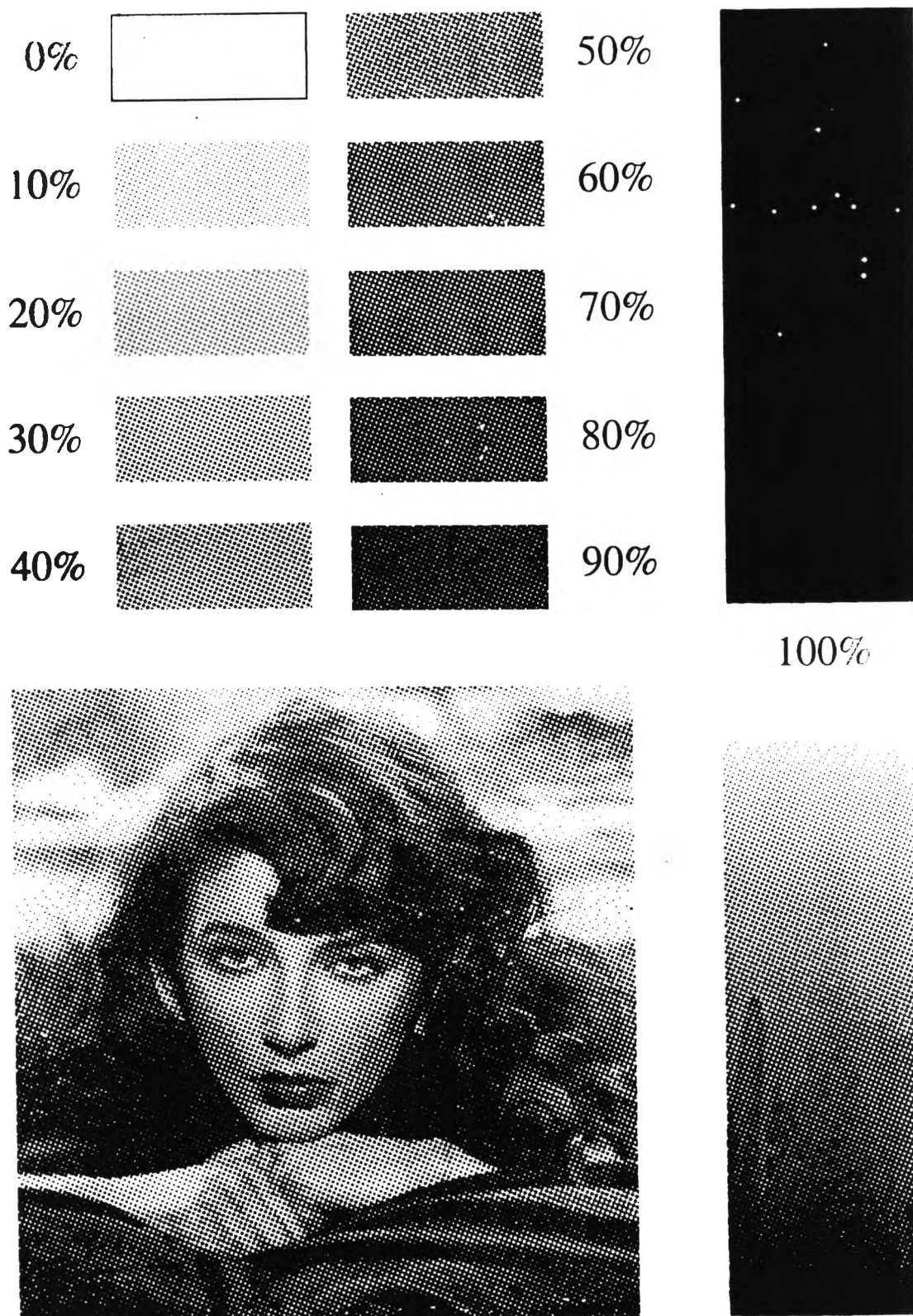


Figure 4.29 Printed image on the treated CPP film after seven days of storage time, printed with the ink I

Screen 30 lpi

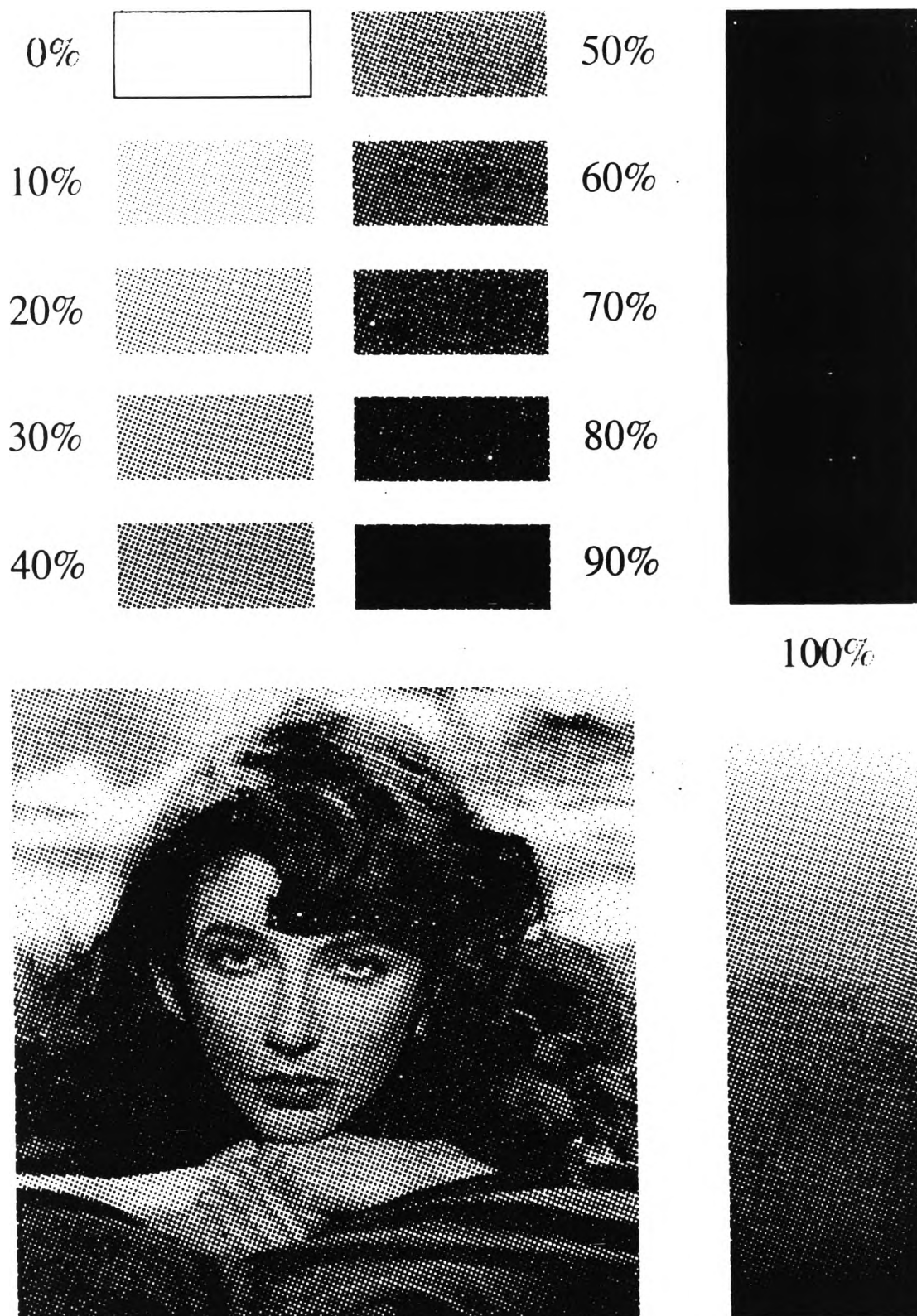


Figure 4.30 Printed image on the treated CPP film after fourteen days of storage time, printed with the ink I

Screen 30 lpi

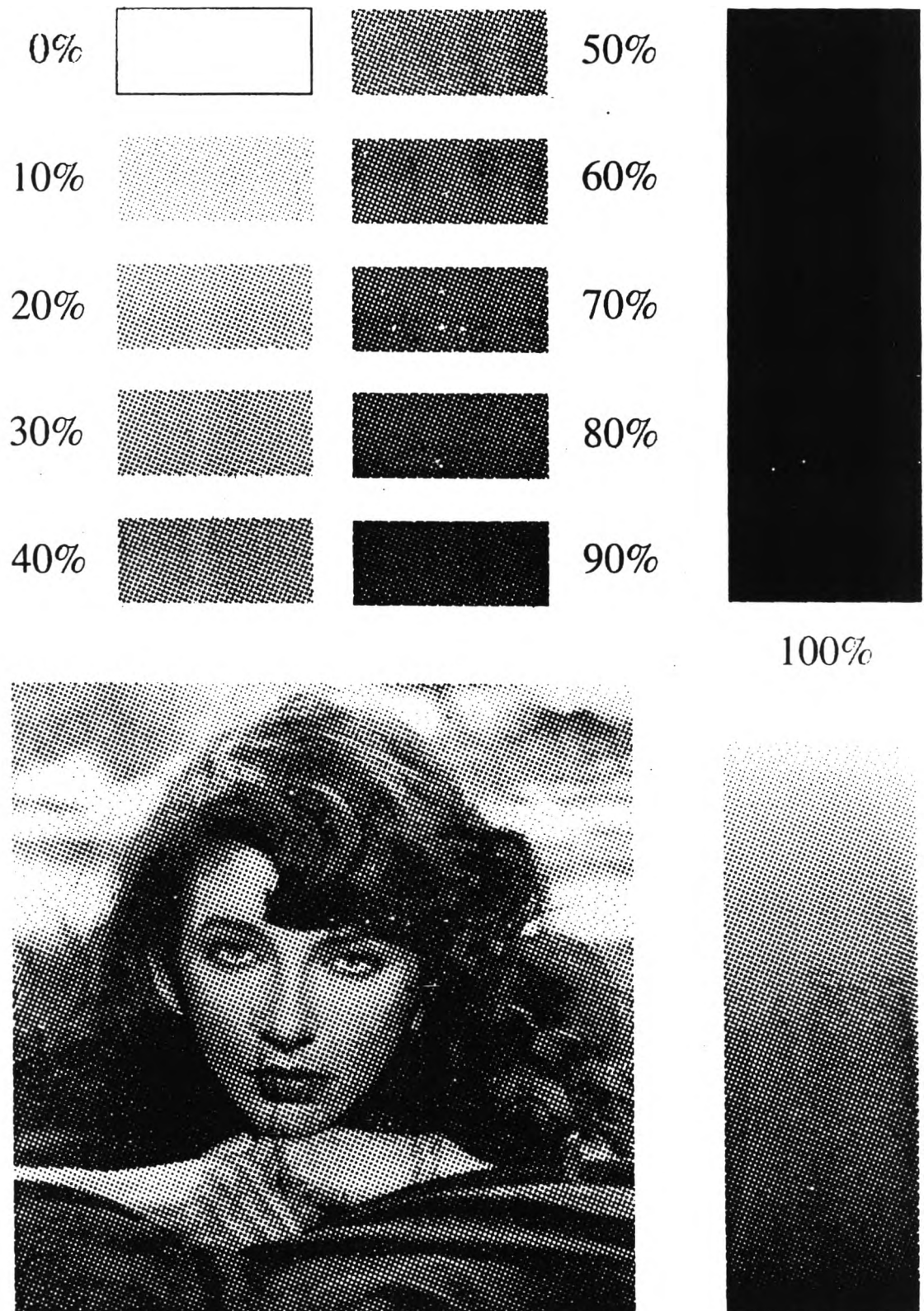


Figure 4.31 Printed image on the freshly treated CPP film printed with the ink II

Screen 30 lpi

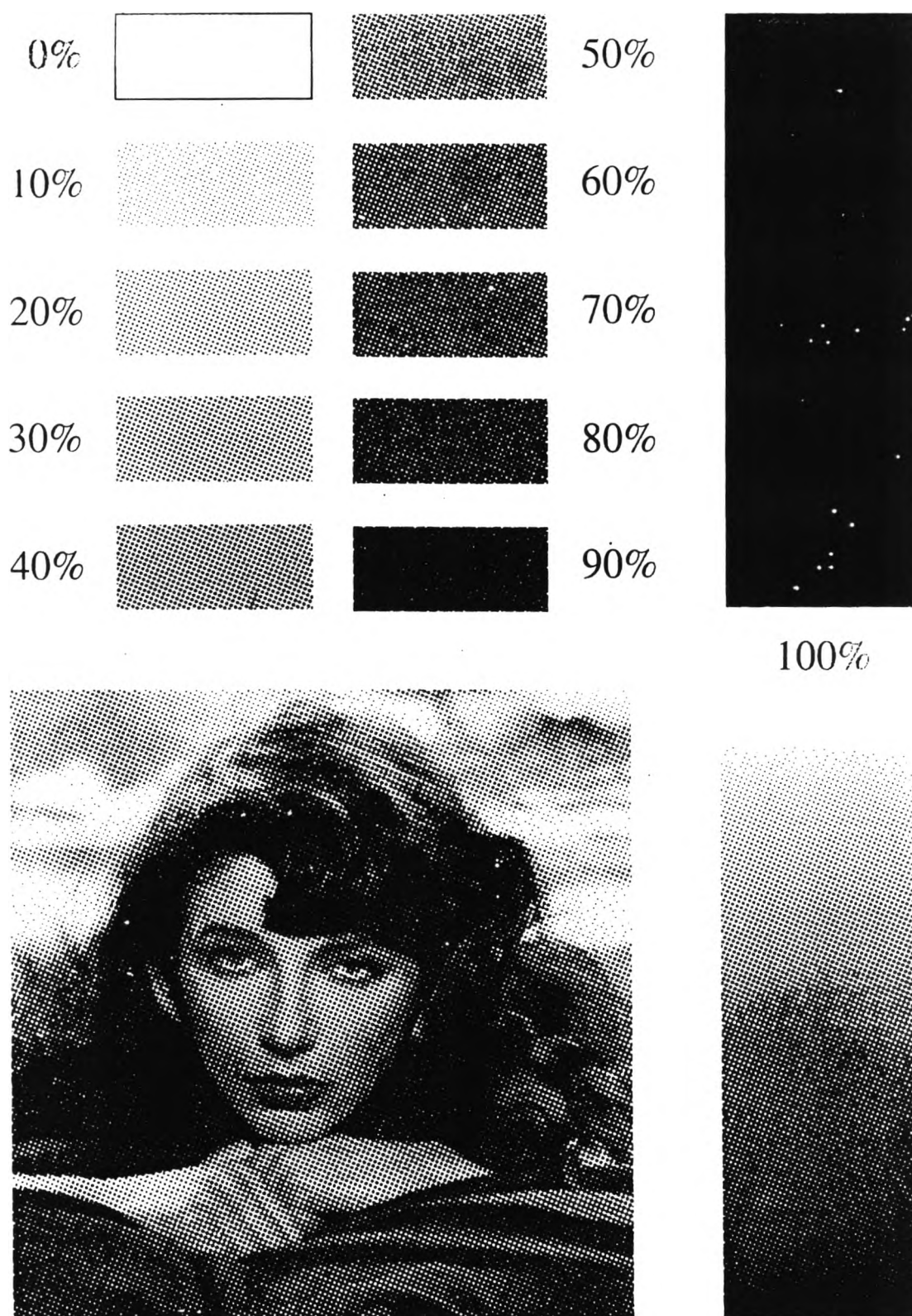


Figure 4.32 Printed image on the treated CPP film after seven days of storage time, printed with the ink II

Screen 30 lpi

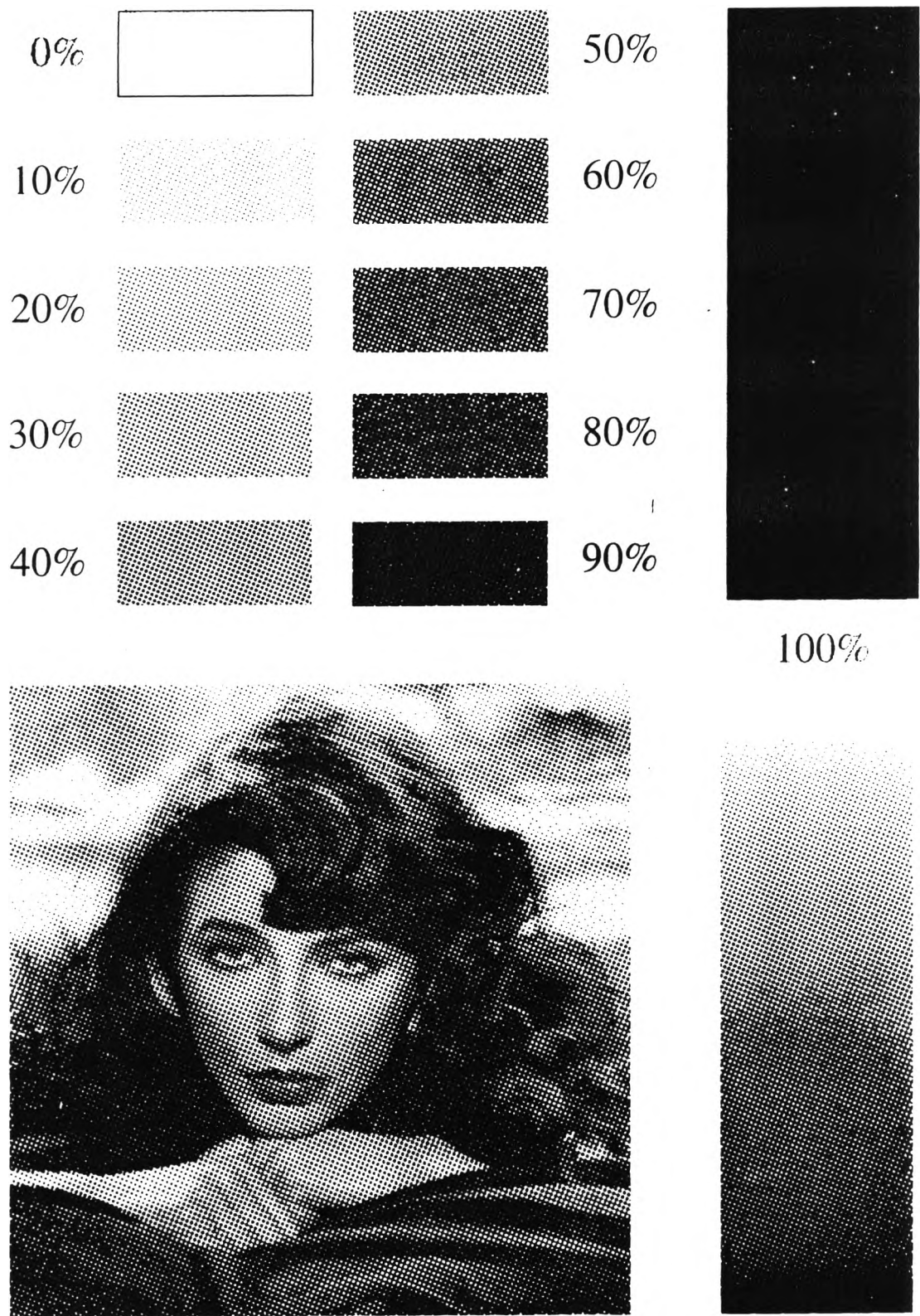


Figure 4.33 Printed image on the treated CPP film after fourteen days of storage time, printed with the ink II

Table 4.18 % Dot Area and Dot Gain of Plastic Films Printed with Ink I for Various Storage Times

% Dot Area of Original Film	% Dot of Printed Plastic Film			% Dot Gain		
	Storage Time before Printing (days)			Storage Time before Printing (days)		
	0	7	14	0	7	14
10	10	8	8	0	-2	-2
20	25	24	25	5	4	5
30	40	36	37	10	6	7
40	51	47	50	11	7	10
50	56	52	57	6	2	7
60	71	66	71	11	6	11
70	78	74	76	8	4	6
80	86	83	85	6	3	5
90	93	91	92	3	1	2
100	100	99	100	0	-1	0

Table 4.19 % Dot Area and Dot Gain of Plastic Films Printed with Ink II for Various Storage Times

% Dot Area of Original Film	% Dot of Printed Plastic Film			% Dot Gain		
	Storage Time before Printing (days)			Storage Time before Printing (days)		
	0	7	14	0	7	14
10	6	5	5	-4	-5	-5
20	21	17	16	1	-3	-4
30	35	32	29	5	2	-1
40	49	47	41	9	7	1
50	66	56	51	16	6	1
60	77	75	73	17	15	13
70	84	83	81	14	13	11
80	91	90	88	11	10	8
90	96	95	94	6	5	4
100	98	99	99	-2	-1	-1

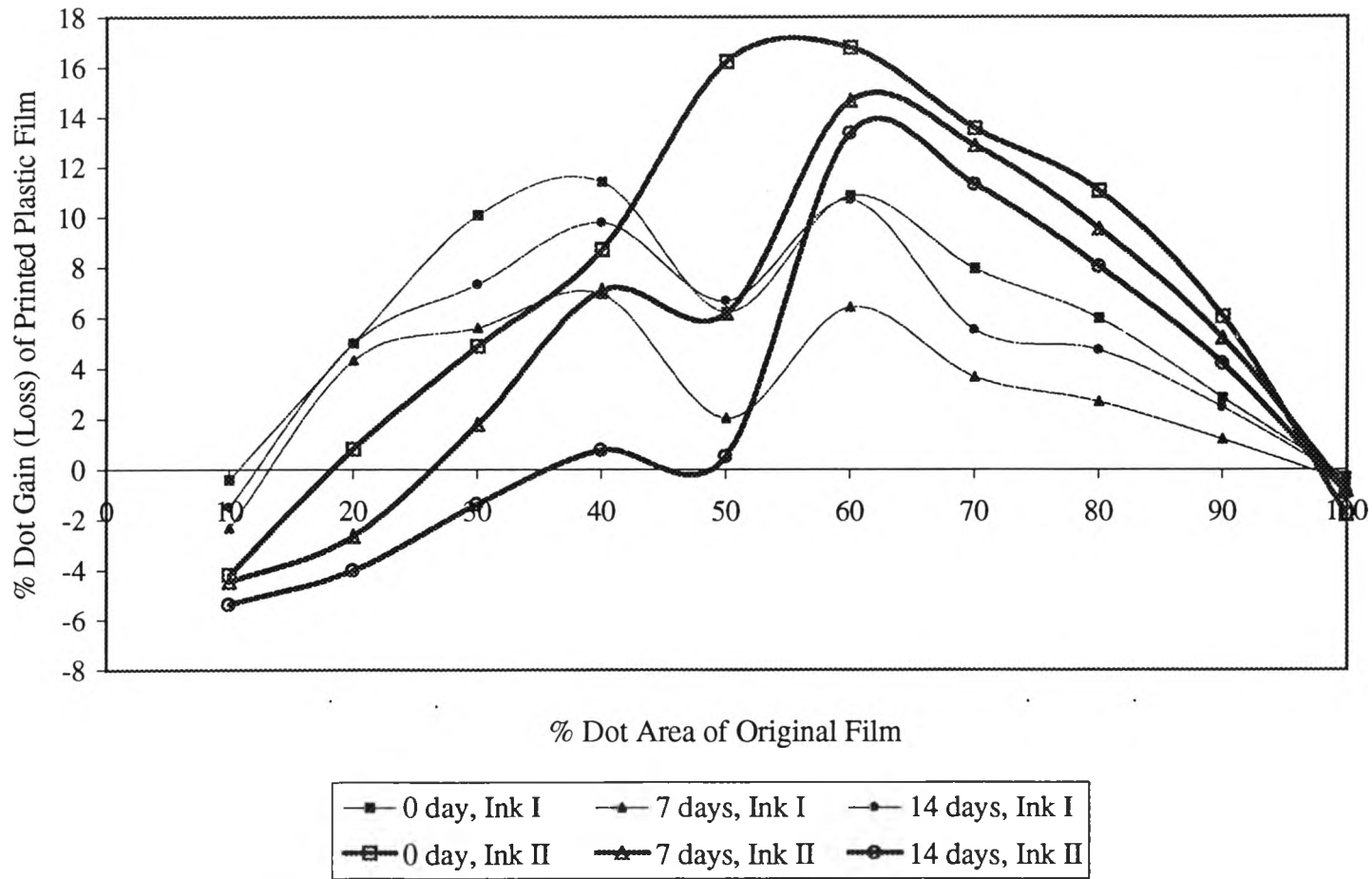


Figure 4.34 % Dot gain of the plastic film printed with ink I and ink II (varying storage times of treated plastic films before printing)

Table 4.20 Tone Reproduction of the Treated CPP Film Printed by Ink I at several Storage Times

% Dot Location	Density of Original Film	Density of Printed Plastic Film		
		Storage Time before Printing (days)		
		0	7	14
0	0.00	0.00	0.00	0.00
10	0.05	0.04	0.03	0.04
20	0.12	0.11	0.09	0.09
30	0.16	0.19	0.16	0.17
40	0.25	0.28	0.23	0.26
50	0.34	0.30	0.27	0.30
60	0.42	0.43	0.39	0.41
70	0.52	0.51	0.48	0.50
80	0.71	0.67	0.62	0.64
90	1.03	0.84	0.83	0.82
100	4.29	1.20	1.26	1.17

Varying Storage Times of Treated Plastic Film for 0, 7, and 14 Days before Printing

Table 4.21 Tone Reproduction of the Treated CPP Film Printed by Ink II at several Storage Times

% Dot Location	Density of Original Film	Density of Printed Plastic Film		
		Storage Time before Printing (days)		
		0	7	14
0	0.00	0.00	0.00	0.00
10	0.05	0.02	0.03	0.02
20	0.12	0.08	0.07	0.07
30	0.16	0.16	0.14	0.13
40	0.25	0.25	0.23	0.21
50	0.34	0.35	0.30	0.26
60	0.42	0.48	0.43	0.44
70	0.52	0.59	0.56	0.57
80	0.71	0.76	0.72	0.75
90	1.03	0.94	0.90	0.97
100	4.29	1.25	1.24	1.35

Varying Storage Times of Treated Plastic Film for 0, 7, and 14 Days before Printing

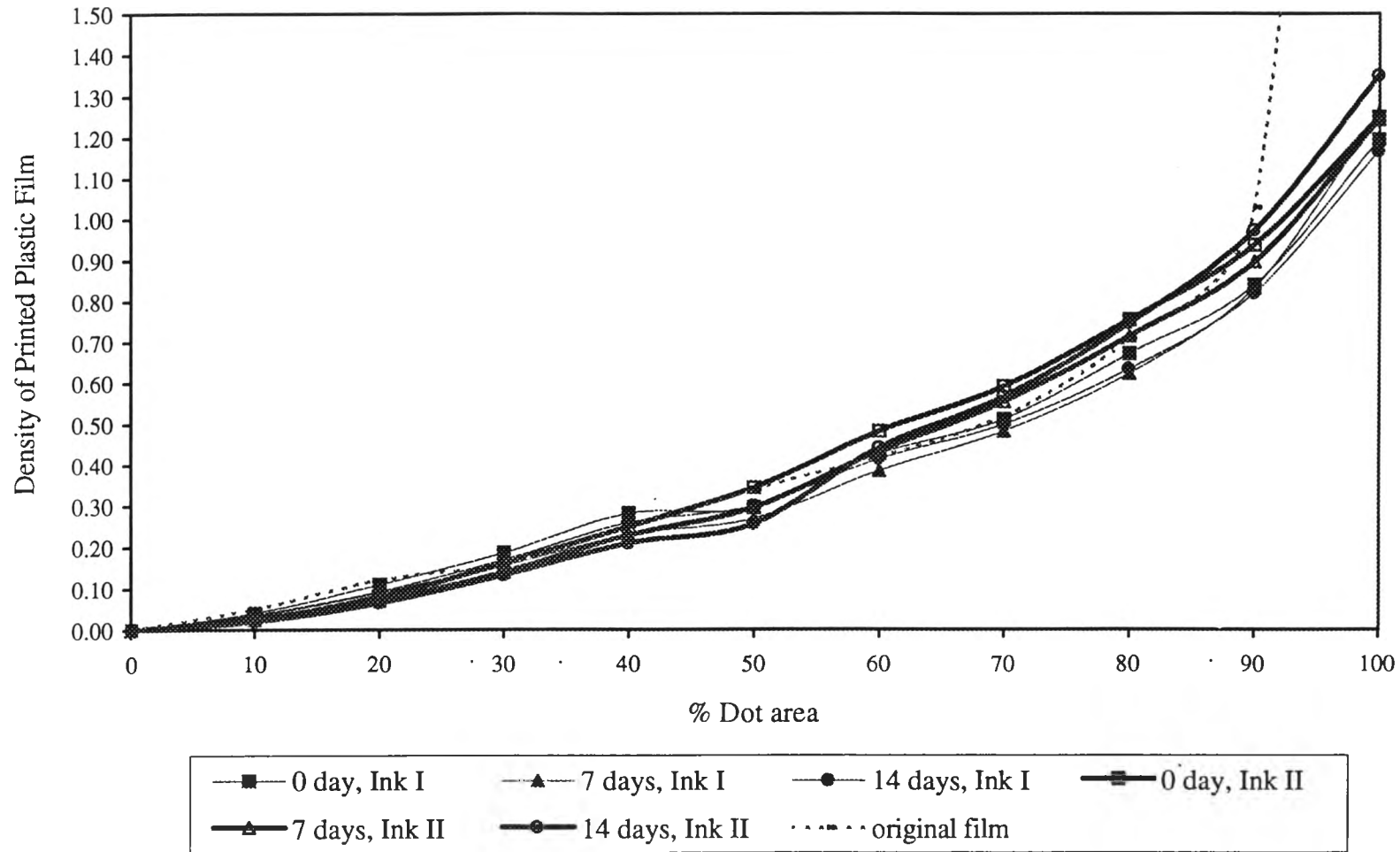


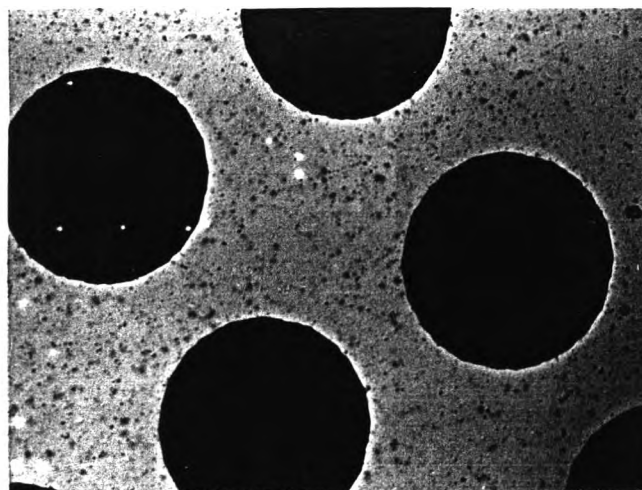
Figure 4.35 Density of the plastic films printed with ink I and ink II (varying storage times of treated plastic films before printing)

c) Dot Characteristics

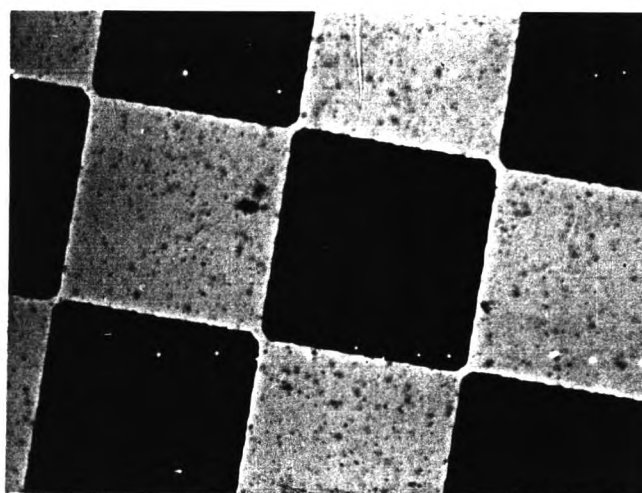
Dot characteristics of the original film and the printed plastic film were compared. Dot Characteristics at 40, 50 and 60% dot area of original film and the unstorage, treated plastic film printed by ink I and ink II are shown Figures 4.36-4.38. Considering the halftone dots at 40, 50, and 60% area, the ink coverage of 40 and 50% dot area printed by ink II is somewhat better than those produced by ink I. However, the dot shape especially the round dots is more spread than the square dots. At 60% dot area, the ink coverage by both inks are very bad. Ink spreading into the non-image areas is the major defects of the flow behavior. We could possibly state that the viscosity of the two inks might not be high enough to prevent ink spreading and feathering. Nonetheless, ink I could print the 60% dot area more even than could the ink II, because, ink I had a higher ink viscosity and it does not contain silicone defoamer. More evidence is observed in Figure 4.39 where the shadow area printed by ink I are more uniform than those of ink II, even though both inks produced some pinholes. One more important characteristic being observed about ink dispersion is the degree of pigment dispersion. Both inks contained some amount of oversized pigment particles, which were shown markedly in the print of ink I. A lesser extent of poor pigment dispersion was also seen in Figure 4.39 (b).

d) % Print Contrast

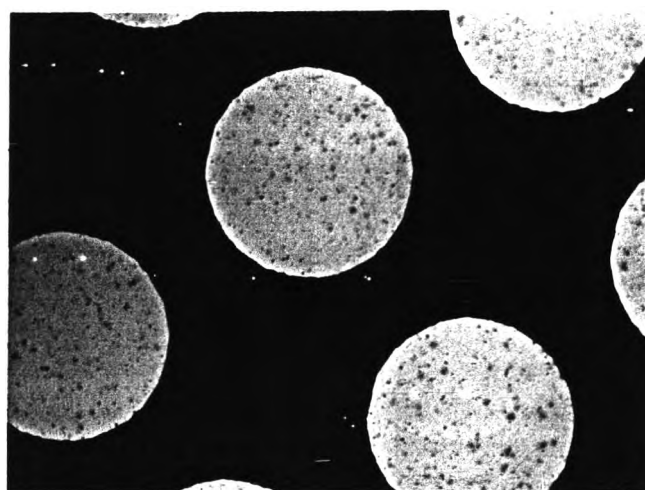
The print contrast is often determined by subtracting the printed density tint from the printed density of a solid and dividing by the solid ink density. The print contrast determines dot gain, fill in and slur values [51]. Table 4.22 shows % print contrast of ink I and ink II. It can be seen that % print contrast of the treated plastic film printed by both inks is not significantly different, regardless of ageing.



(a)

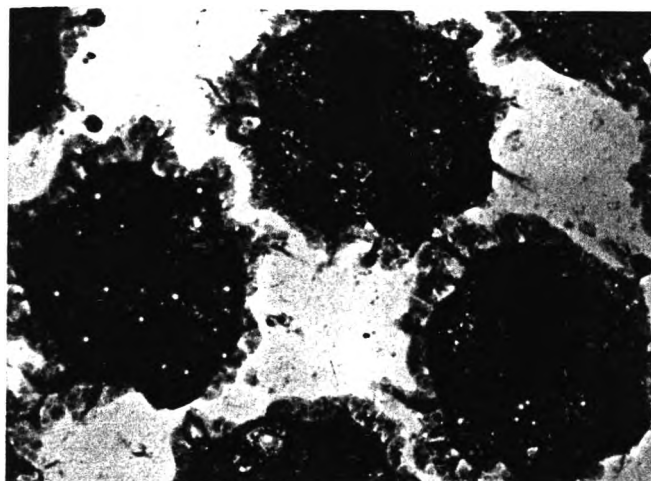


(b)

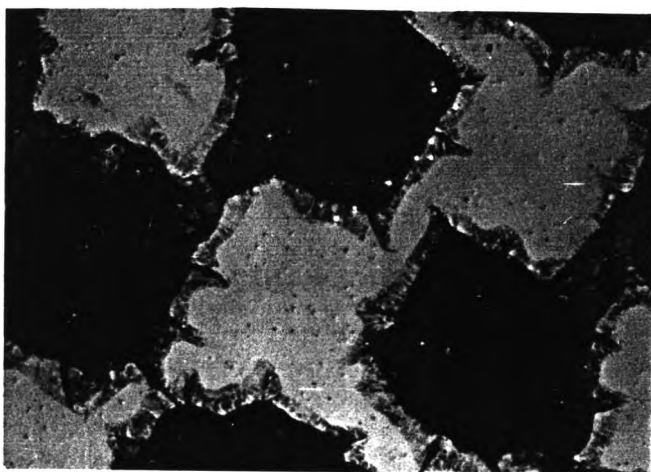


(c)

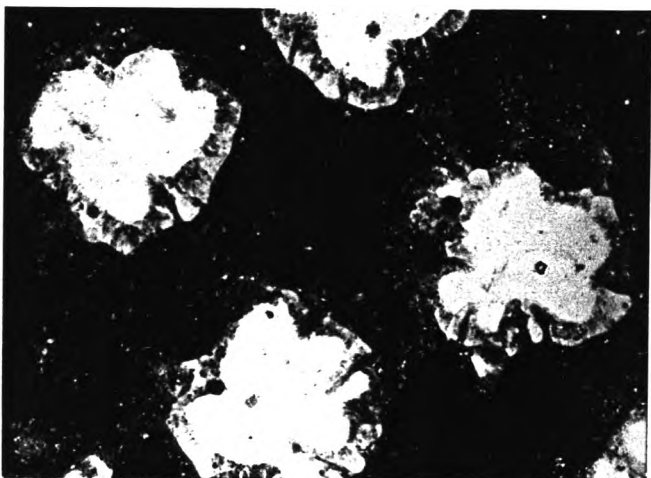
Figure 4.36 Dot characteristics of the original film (a) 40, (b) 50 and (c) 60% dot area



(a)

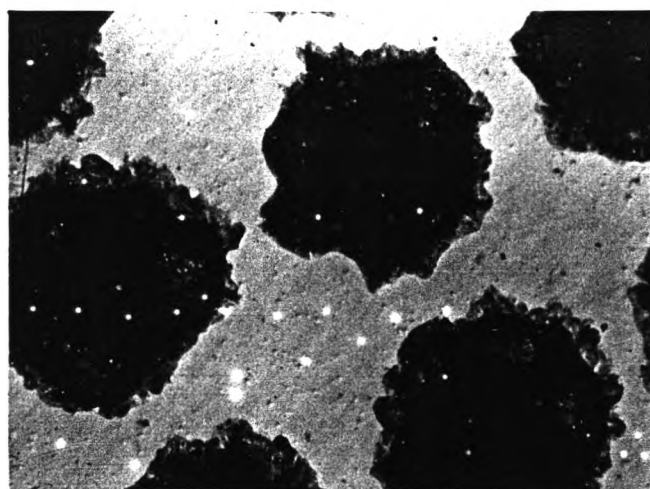


(b)

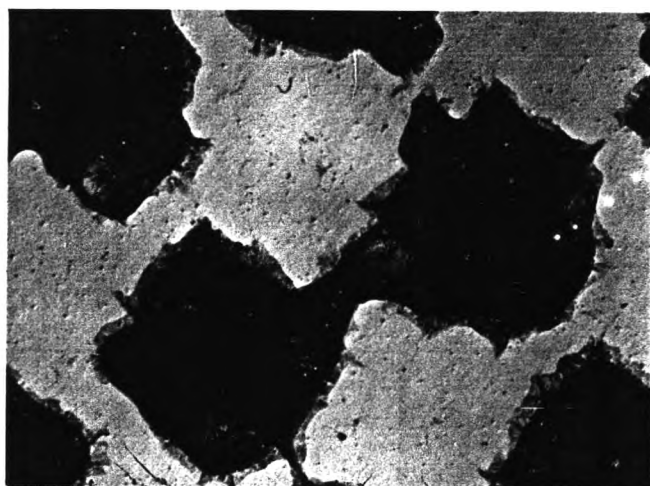


(c)

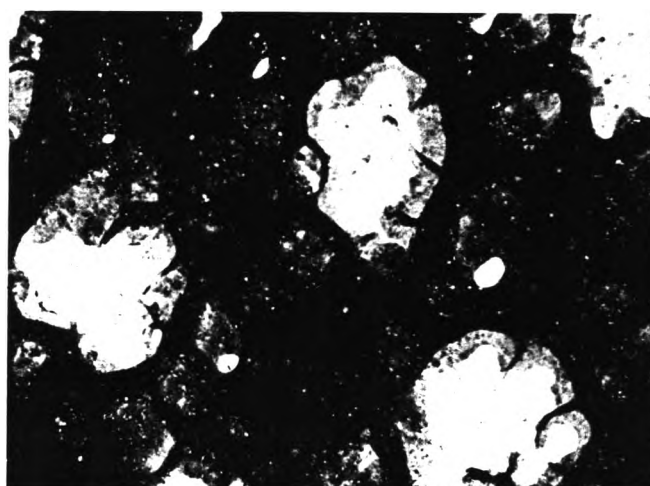
Figure 4.37 Reproduced dot characteristics of the unstorage, treated plastic film printed by ink I (a) 40, (b) 50 and (c) 60% dot area



(a)

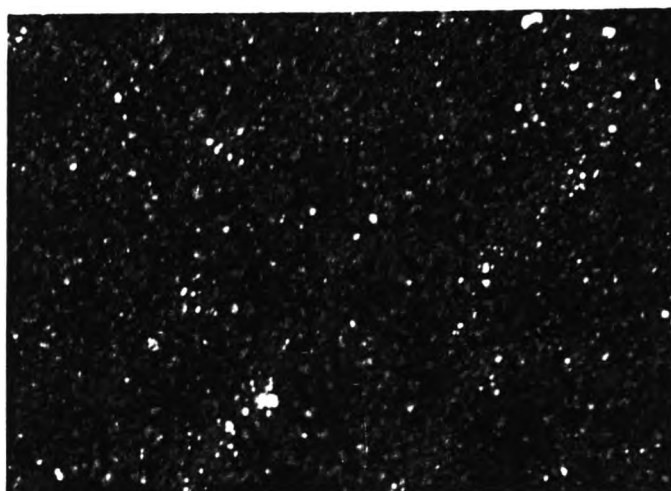


(b)

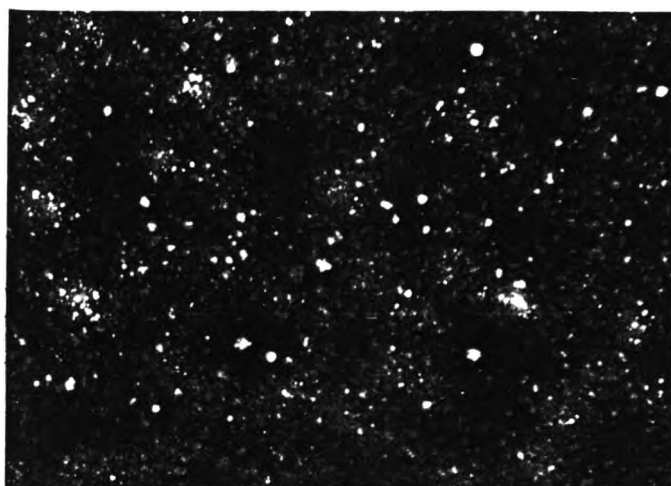


(c)

Figure 4.38 Reproduced dot characteristics of the unstorage, treated plastic film printed by ink II (a) 40, (b) 50 and (c) 60% dot area



(a)



(b)

Figure 4.39 Shadow area of the unstorage, treated plastic film printed by ink I (a) and ink II (b)

Basically, the highest print contrast indicates the minimum dot gain. On the other hand, the lowest print contrast presents the minimum dot gain. Although the results of dot gain in print by ink II are relatively higher at mid-tone dots, we still cannot conclude that the slightly difference in print contrast is caused by the effect of dot gain.

Table 4.22 % Print Contrast of the Printed Plastic Film with Various Storage Times before Printing

Reproduction	% Print Contrast
Ink I, (after treatment)	57 ± 2
Ink I, (7 days)	62 ± 3
Ink I, (14 days)	57 ± 2
Ink II (after treatment)	53 ± 4
Ink II, (7 days)	55 ± 3
Ink II, (14 days)	58 ± 3

e) Gloss

Gloss is a measure of the degree of reflectance on the surface of the print [47]. Table 4.23 shows gloss of the printed plastic films with various storage times before printing. The results show that the plastic film printed by ink II gives the higher gloss than that printed by ink I. The gloss indicates that a better pigment dispersion of ink II was obtained. The finer the pigment particles, the higher the reflectance. The appropriate thickener base can wet the pigment particle surface to exclude the entrapped air and replace the interphase with the molecules of the thickener. This

process eases the milling stage in terms of finer pigment particles, adequate ink flow and full coverage on both dot and solid areas.

We would suggest that some flow reducing additive, levelling agent, and antispreading agent be added into both inks. We should also check for the treatment evenness of the CPP film to ensure a proper surface behavior/interaction with these inks.

Table 4.23 Gloss of the Printed Plastic Film with Various Storage Times before Printing

Reproduction	Gloss ^a
Ink I, (after treatment)	3.2 ± 0.26
Ink I, (7 days)	3.5 ± 0.33
Ink I, (14 days)	3.6 ± 0.27
Ink II (after treatment)	4.4 ± 0.22
Ink II, (7 days)	4.5 ± 0.43
Ink II, (14 days)	4.3 ± 0.32

^aSample size: 30

To observe the difference in gloss values, probability tests of each ink pairs at different treatment condition were further conducted. The tests were evaluated at the confident level of 95% (or $\alpha = 0.05$). The test results show as follows:

Table 4.24 Significant Test in Gloss Value of the Two Inks

Pair Studied / Condition	Significant Value
Ink I – Ink II / after treatment	9.16×10^{-80}
Ink I – Ink II / 7-day storage	2.33×10^{-39}
Ink I – Ink II / 14-day storage	2.13×10^{-34}

Although the gloss values are not inevitably different through visual assessment, the statistical evaluation shows they are significantly different.

f) Adhesion Test

The adhesion of the printed plastic film was evaluated. Figures 4.40-4.45 show the results of adhesion test. Adhesion test results of the plastic film printed by ink I show that the percent area removed is in range of 15-35%, while those of the plastic film printed by ink II is in range of 35-65%. So, the adhesion of the treated plastic film printed by ink I is much better than that printed by ink II.

The extent of corona charger on the treated CPP film and the composition of the ink are responsible for this observation. As mentioned in Table 4.17 for the work of adhesion that the ink I has a relatively higher work of adhesion (67 mN m^{-1}) than that of ink II (61 mN m^{-1}). In addition, the percentage polarity of the CPP treated film by 350 watt was 73% or 30.2 mN m^{-1} , while the total surface energy as 41.2 mN m^{-1} . The surface tension of ink I and ink II were 34 and 32 mN m^{-1} , respectively, which gave a closed wetting behavior (contact angle) of the plastic film.

Screen 30 lpi

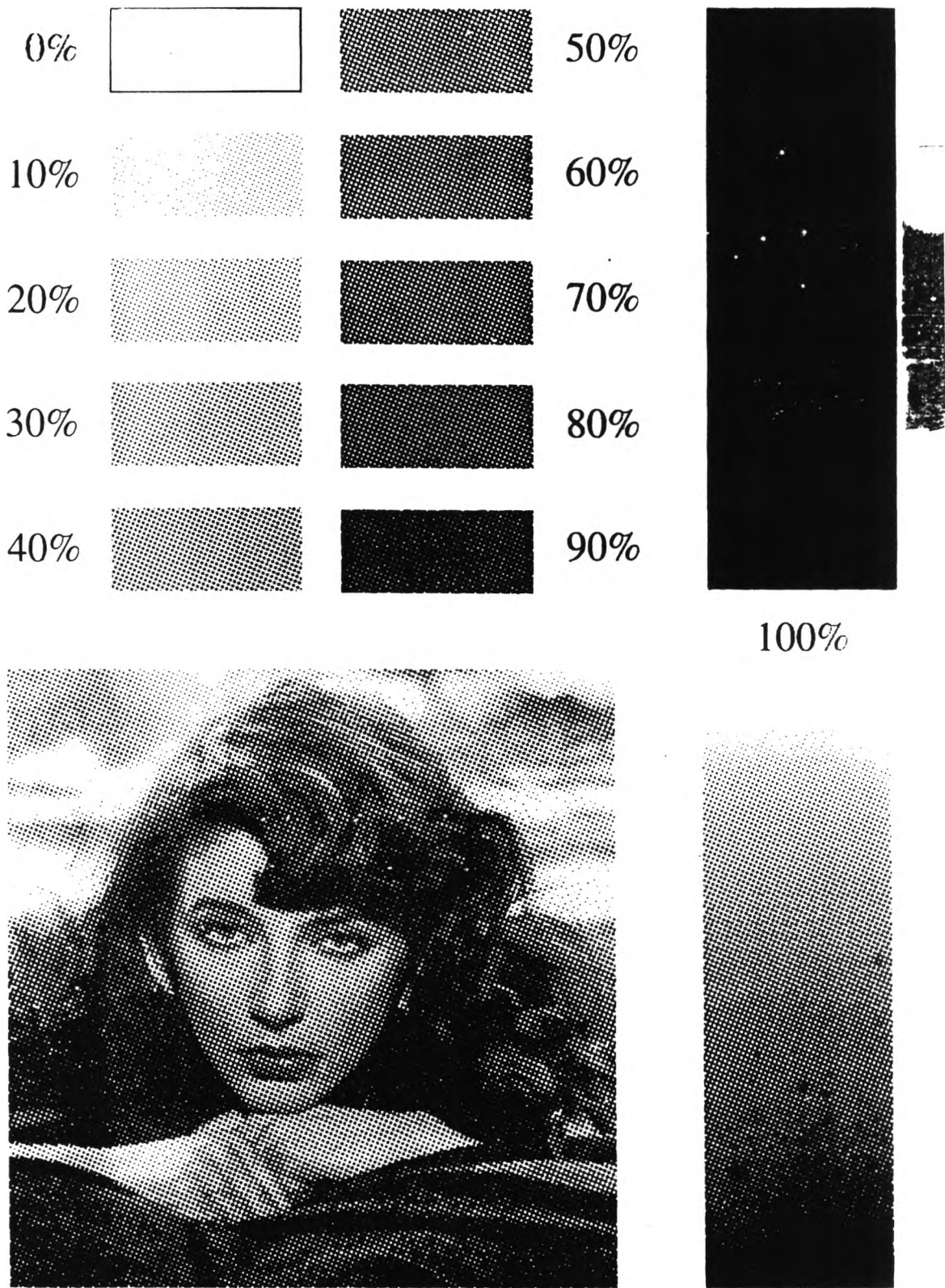


Figure 4.40 Adhesion test result of the unstorage, treated plastic film printed by ink I

Screen 30 lpi

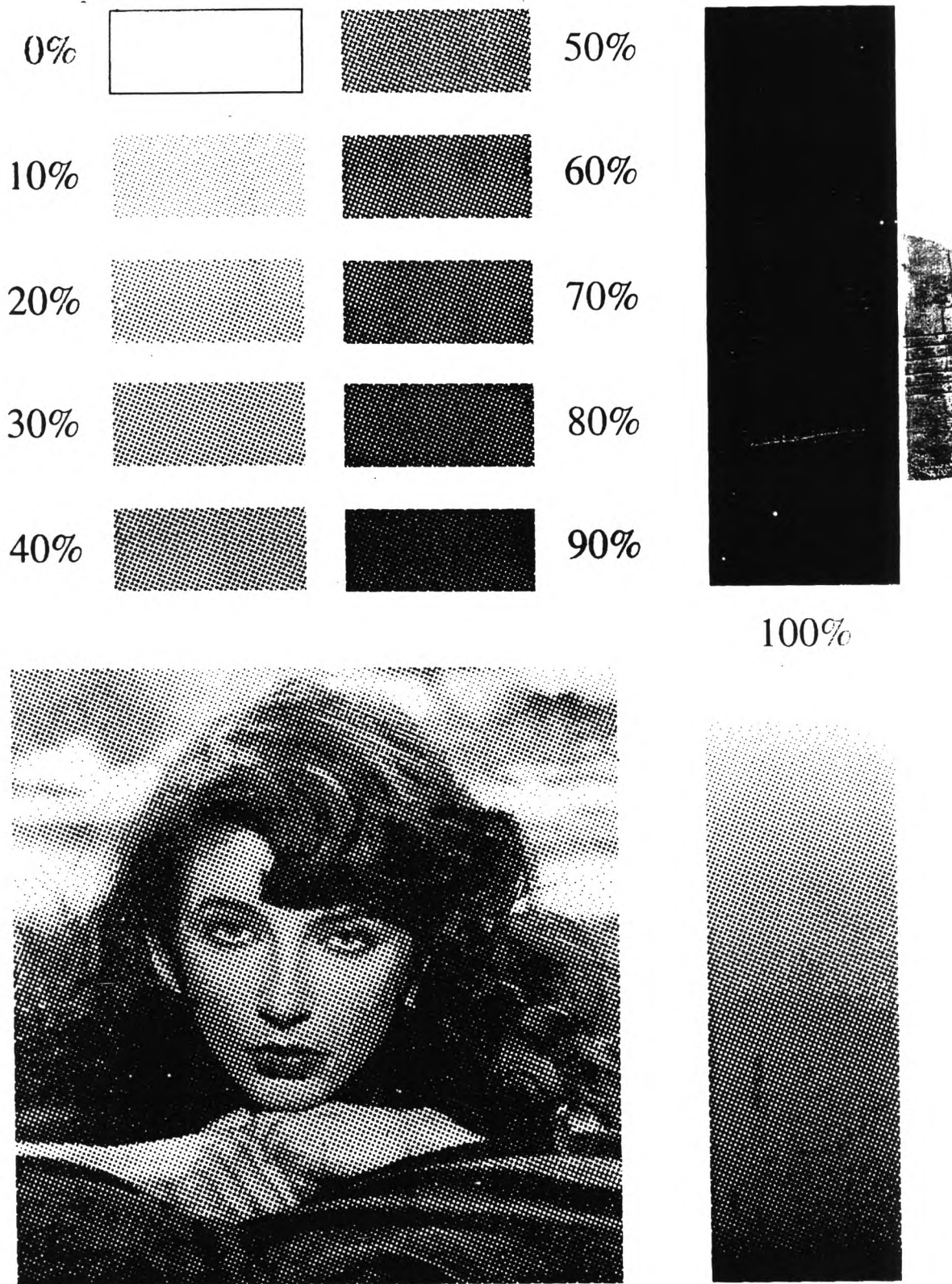


Figure 4.41 Adhesion test result of the 7-day stored, treated plastic film printed by ink I

Screen 30 lpi

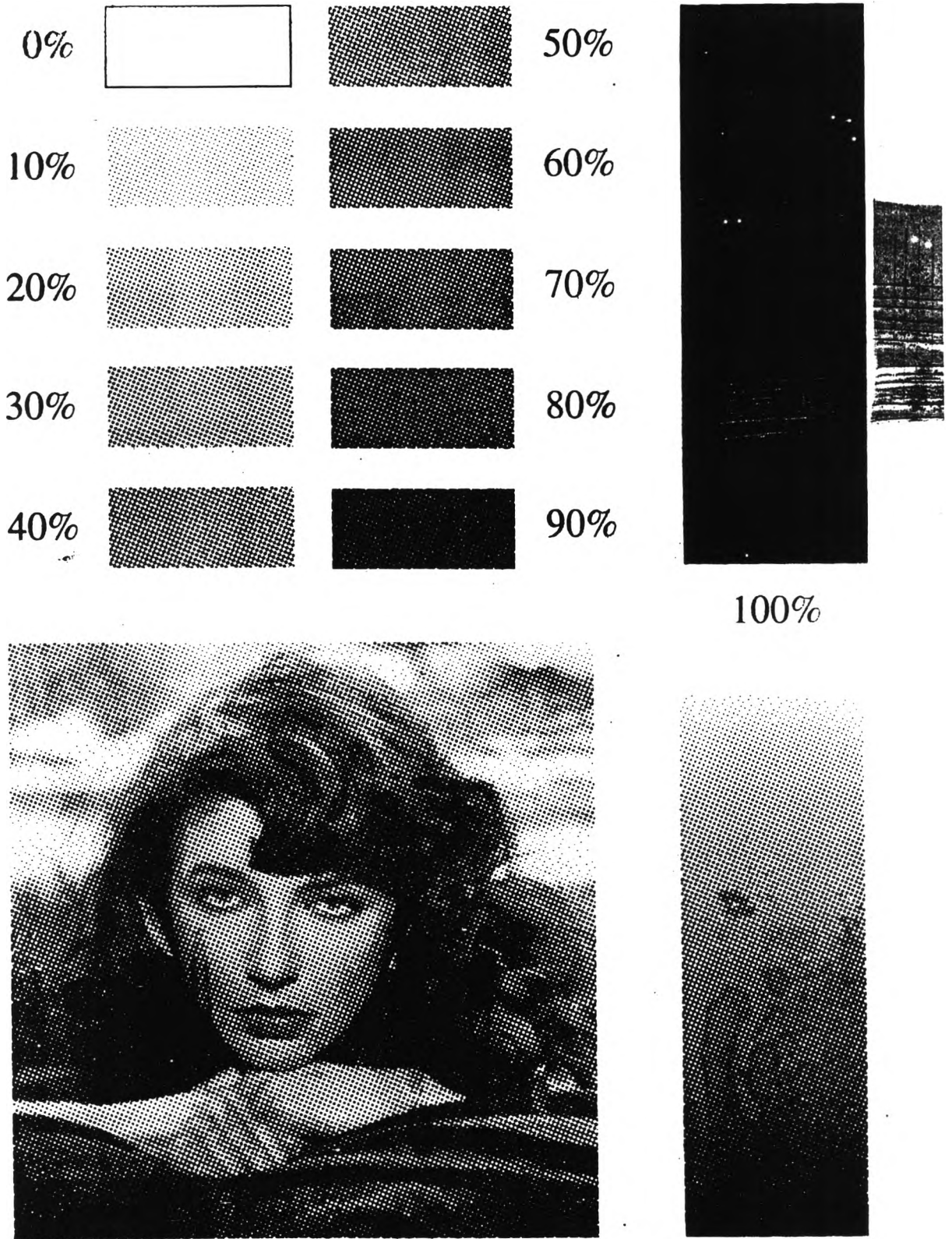


Figure 4.42 Adhesion test result of the 14-day stored, treated plastic film printed by ink I

Screen 30 lpi

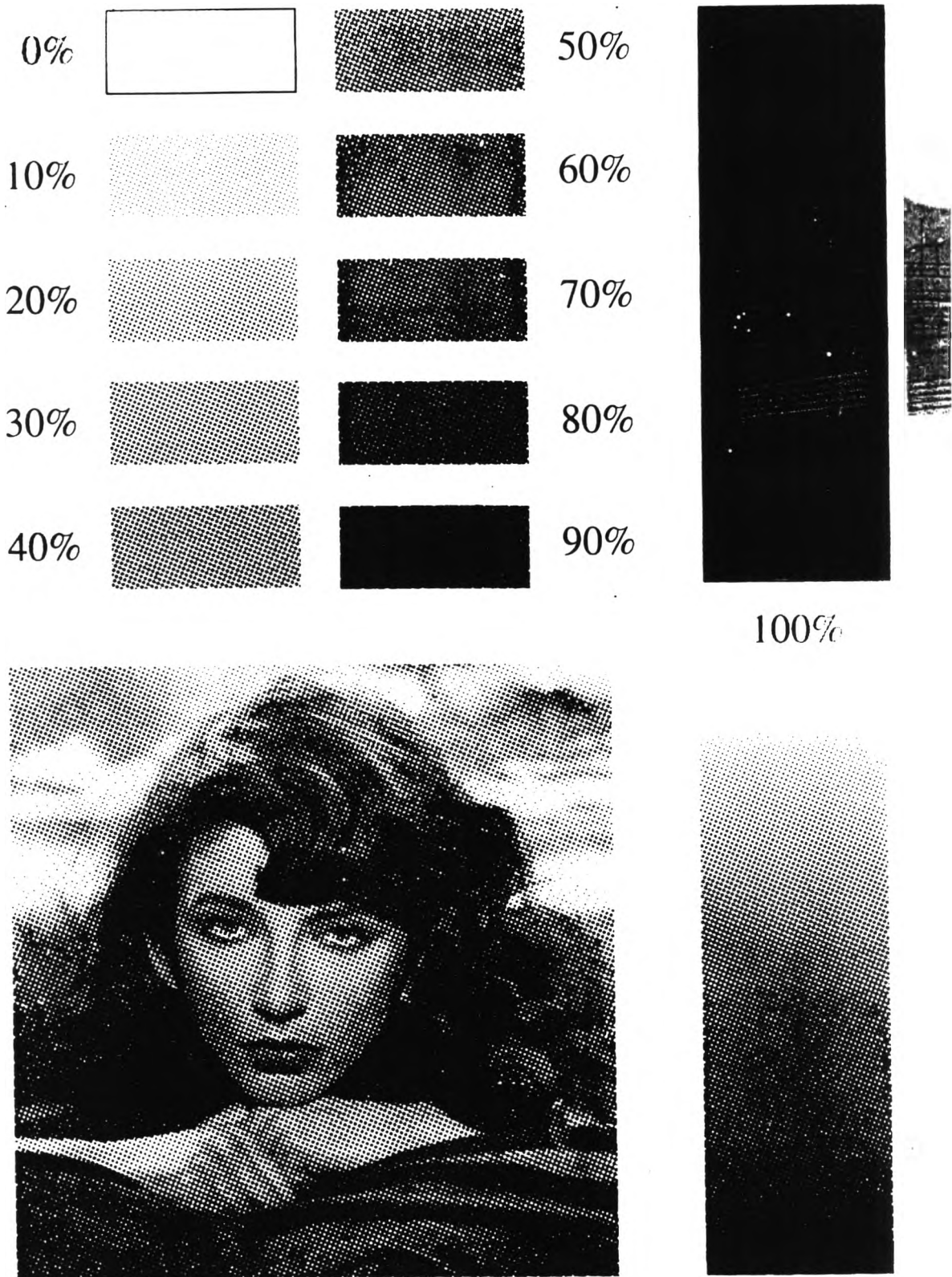


Figure 4.43 Adhesion test result of the unstorage, treated plastic film printed by ink II

Screen 30 lpi

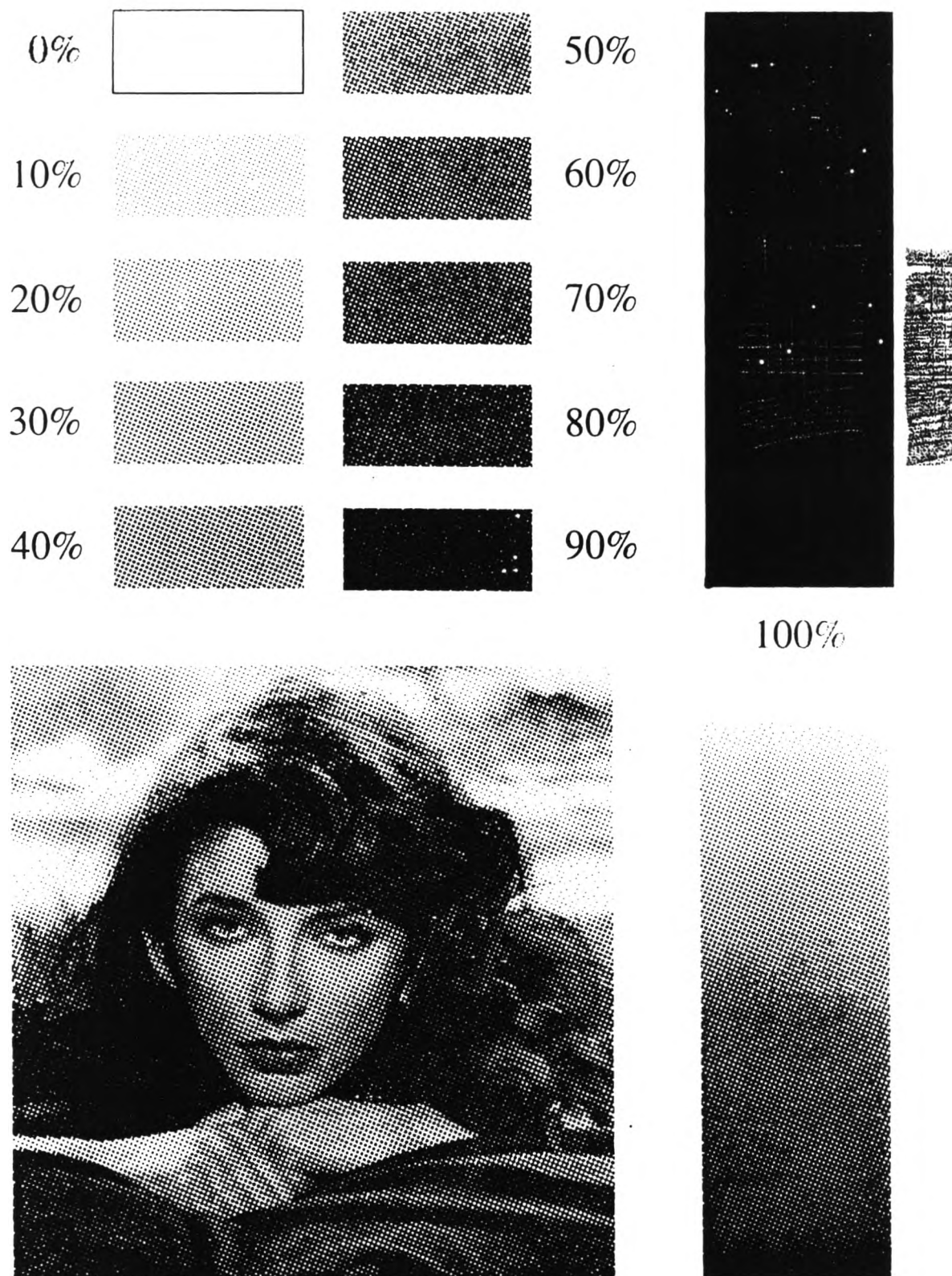


Figure 4.44 Adhesion test result of the 7-day stored, treated plastic film printed by ink II

Screen 30 lpi

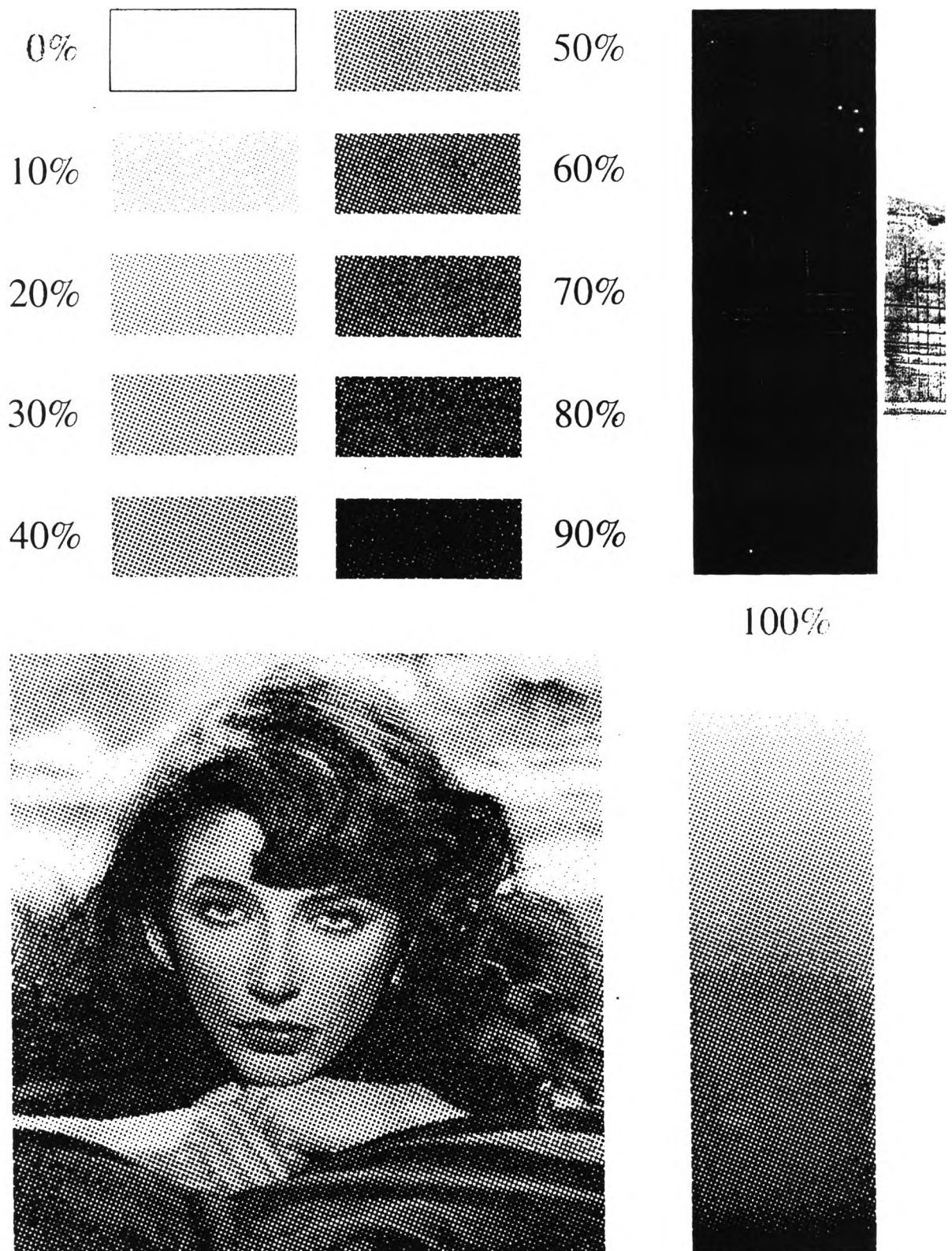


Figure 4.45 Adhesion test result of the 14-day stored, treated plastic film printed by ink II